

Simultaneous Conversion of Dialkyl Phosphites to Dialkylphosphoric Acids and SeO₂ to Se Nanoparticles in Water and their Anti-cancer Properties

Babak Kaboudin,^{*a} Hesam Esfandiari,^a Ali Sabzalipour,^a Zahra Oushyani Roudsari,^b

Fahimeh Varmaghani,^a Tianjian Zhang,^c Yanlong Gu,^c

^aDepartment of Chemistry, Institute for Advanced Studies in Basic Sciences (IASBS), Gava Zang, Zanjan 45137-66731, Iran

^bDepartment of Medical Biotechnology, School of Medicine, Zanjan University of Medical Sciences, Zanjan, Iran

^cSchool of Chemistry and Chemical Engineering, Huazhong University of Science & Technology, Wuhan 430074, China

^{*}Corresponding authors, Tel: +98 24 33153220; Fax: +98 24 33153232. E-mail address: kaboudin@gmail.com and kaboudin@iasbs.ac.ir;

[Table of Contents](#)

Table S1: Conversion of diethyl phosphite 1a to diethyl phosphate 2a at various conditions	S5
Experimental details, Characterization data of the products	S6-S9
NMR Spectra for the compounds	S10-S54
Figure S1: ¹H NMR Spectra of 2a	
Figure S2: ¹³C NMR Spectra of 2a	

Figure S3: ^{31}P NMR Spectra of 2a

Figure S4: ^1H NMR Spectra of 2b

Figure S5: ^{13}C NMR Spectra of 2b

Figure S6: ^{31}P NMR Spectra of 2b

Figure S7: ^1H NMR Spectra of 2c

Figure S8: ^{13}C NMR Spectra of 2c

Figure S9: ^{31}P NMR Spectra of 2c

Figure S10: ^1H NMR Spectra of 2d

Figure S11: ^{13}C NMR Spectra of 2d

Figure S12: ^{31}P NMR Spectra of 2d

Figure S13: ^1H NMR Spectra of 2e

Figure S14: ^{13}C NMR Spectra of 2e

Figure S15: ^{31}P NMR Spectra of 2e

Figure S16: ^1H NMR Spectra of 2f

Figure S17: ^{13}C NMR Spectra of 2f

Figure S18: ^{31}P NMR Spectra of 2f

Figure S19: ^1H NMR Spectra of 2h

Figure S20: ^{13}C NMR Spectra of 2h

Figure S21: ^{31}P NMR Spectra of 2h

Figure S22: ^1H NMR Spectra of 2i

Figure S23: ^{13}C NMR Spectra of 2i

Figure S24: ^{31}P NMR Spectra of 2i

Figure S25: ^1H NMR Spectra of 2j

Figure S26: ^{13}C NMR Spectra of 2j

Figure S27: ^{31}P NMR Spectra of 2j

Figure S28: ^1H NMR Spectra of 2k

Figure S29: ^{13}C NMR Spectra of 2k

Figure S30: ^{31}P NMR Spectra of 2k

Figure S31: ^1H NMR Spectra of 2l

Figure S32: ^{13}C NMR Spectra of 2l

Figure S33: ^{31}P NMR Spectra of 42l

Figure S34: ^1H NMR Spectra of 2m

Figure S35: ^{13}C NMR Spectra of 2m

Figure S36: ^{31}P NMR Spectra of 2m

Figure S37: ^1H NMR Spectra of 2n

Figure S38: ^{13}C NMR Spectra of 2n

Figure S39: ^{31}P NMR Spectra of 2n

Figure S40: ^1H NMR spectra of 3

Figure S41: ^{13}C NMR spectra of 3

Figure S42: ^{31}P NMR spectra of 3

Figure S43: ^1H NMR spectra of **4**

Figure S44: ^{13}C NMR spectra of **4**

Figure S45: ^{31}P NMR spectra of **4**

Figure S46: TEM images of DMP-Se-NPs S55

Figure S47: Ultraviolet–visible of DMP-Se-NPs S56

Figure S48: XPS analysis of DMP-Se-NPs S57

Figure S49: FE-SEM image of β -CD@Se NPs S58

Figure S50: TEM of a sample of aggregated Se-NPs

Figure S51: Cell viability after treatment with different concentrations of Se NPs (2.5, 5, 10, 20, 40, 80 and 160 $\mu\text{g}/\text{ml}$) after 24 h for **A.** 4T1 **B.** MCF-7 and **C.** MDA-MB-231 cells. Data is represented as mean \pm SD. SD: standard deviation. (magnification \times 100).

Figure S52: Cyclic voltammograms of (a and b) 50 mM SeO_2 at different ranges of potential and (c) 100 mM diethylphosphite at glassy carbon electrode in water containing 0.1 M KCl at scan rate of 100 mV/s. The cross indicates the starting potential. The arrows show the direction of the potential scan. S59-S64

Figure S53: ^{31}P NMR Spectra of the conversion of the compound **1a** to **2a** in the presence of SeO_2 in D_2O at rt S65

Figure S54 The reaction mixture of SeO_2 (0.5 mmol) diethylphosphite (1 mmol) with other stabilizers in water after 2h at 60 $^\circ\text{C}$

Table S1: Conversion of diethyl phosphite 1a to diethyl phosphate 2a at various conditions

Entry	Phosphite (mmol)	Oxidant(mmol)	T (°C)	Time (h)	solvent	Yield(%)
1	0.5	SeO ₂ 0.25	rt	12	DMSO	90
2	0.5	SeO ₂ 0.25	rt	12	DMF	54
3	0.5	SeO ₂ 0.25	rt	12	H ₂ O	Quant.
4	0.5	SeO ₂ 0.25	rt	12	MeOH	63
5	0.5	SeO ₂ 0.25	rt	12	Acetonitrile	90
6	0.5	SeO ₂ 0.25	rt	6	Acetonitrile	90
7	0.5	SeO ₂ 0.25	rt	12	Dioxane	89
8	0.5	SeO ₂ 0.25	rt	12	CH ₂ Cl ₂	87
9	0.5	SeO ₂ 0.25	rt	12	n-Hexane	83
10	0.5	SeO ₂ 0.25	rt	12	CHCl ₃	80
11	0.5	Na ₂ SeO ₃ 0.25	rt	12	H ₂ O	--
12	0.5	H ₂ O ₂	rt	12	H ₂ O	--
13	0.5	O ₂	rt	12	H ₂ O	--
14	0.5	--	rt	12	H ₂ O	--
15	0.5	SeO ₂ 0.5	rt	12	H ₂ O	Quant.
16	1.00	SeO ₂ 0.25	rt	12	H ₂ O	45
17	0.5	SeO ₂ 0.25	rt	6	H ₂ O	Quant.
18	0.5	SeO ₂ 0.25	rt	3	H ₂ O	Quant.

General: All chemicals were commercial products. NMR spectra were obtained with a 400 MHz Bruker Avance instrument with the chemical shifts being reported as δ ppm and couplings expressed in Hertz. The chemical shift data for each signal on ^1H NMR are given in units of δ relative to CHCl_3 ($\delta=7.26$) for CDCl_3 solution. For ^{13}C NMR spectra, the chemical shifts in CDCl_3 and DMSO are recorded relative to the CDCl_3 resonance ($\delta=77.0$) and DMSO resonance ($\delta=40.45$). Silica gel column chromatography was carried out with Silica gel 100 (Merck No. 10184). Merck Silica-gel 60 F254 plates (No. 5744) were used for the preparative TLC.

General Procedure for the conversion of dialkylphosphite 1 to Dialkylphosphate 2

A solution of selenium dioxide (110 mg, 0.5 mmol) in either water or acetonitrile (4.0 ml) was prepared. Dialkylphosphite or diaryl phosphine oxide **1** (1.0 mmol) was then added to the solution at room temperature under air. The mixture was stirred for 3 hours, during which a red coloration developed, indicating the formation of selenium nanoparticles. The reaction mixture was allowed to stand for an additional 12 hours to facilitate nanoparticle aggregation and growth. Subsequently, the solution was filtered through a 0.45 μm filter to separate the selenium nanoparticles from the solution. Finally, the filtrate was subjected to thermal treatment at 80°C to remove the solvent, yielding the final product **2** without further purification.

Diethyl hydrogen phosphate (2a): The product was obtained as a colourless oil in 94% yield (145 mg, CAS No.: 598-02-7); ^1H NMR (400 MHz, Chloroform-*d*) δ 11.63 (s, 1H), 4.21 – 3.89 (m, 4H), 1.31 (t, $J = 7.0$, 6H); ^{13}C { ^1H } NMR (101 MHz, Chloroform-*d*) δ 63.6 (d, $J = 5.9$ Hz), 15.9 (d, $J = 7.0$ Hz); ^{31}P { ^1H } NMR (162 MHz, Chloroform-*d*) δ -1.34 ppm.

Dimethyl hydrogen phosphate(2b): The product was obtained as a colourless oil in 92% yield (116 mg, CAS No.: 813-78-5); ^1H NMR (400 MHz, Chloroform-*d*) δ 12.36 (s, 1H), 3.84 – 3.72 (d, $J = 11.3$, 6H); ^{13}C { ^1H } NMR (101 MHz, Chloroform-*d*) δ 54.1 (d, $J = 5.9$ Hz) ppm; ^{31}P { ^1H } NMR (162 MHz, Chloroform-*d*) δ 1.55 ppm.

Dibutyl hydrogen phosphate (2c): The product was obtained as colourless oil in 85% yield (155 mg, CAS No.: 107-66-4); ^1H NMR (400 MHz, Chloroform-*d*) δ 12.23 (s, 1H), 4.04 (q, $J = 6.6$ Hz, 4H), 1.68 (m, 4H), 1.54 – 1.19 (m, 4H), 0.95 (t, $J = 7.5$ Hz, 6H). ^{13}C { ^1H } NMR (101 MHz, Chloroform-*d*) δ 67.3 (d, $J = 5.9$ Hz), 32.1 (d, $J = 7.3$ Hz), 18.6, 13.5; ^{31}P { ^1H } NMR (162 MHz, Chloroform-*d*) δ 0.55 pm.

Diisobutyl hydrogen phosphate (2d): The product was obtained as a colourless oil in 97% yield (204 mg, CAS No.: 6303-30-6); ^1H NMR (400 MHz, DMSO-*d*₆) δ 9.20 (s, 1H), 3.67 (t, $J = 6.5$ Hz, 4H), 1.88 (dp, $J = 13.3$, 6.6 Hz, 2H), 0.92 (d, $J = 6.8$ Hz, 12H). ^{13}C { ^1H } NMR (101 MHz, DMSO) δ 72.3 (d, $J = 6.0$ Hz), 29 (d, $J = 7.1$ Hz), 18.9 ppm; ^{31}P { ^1H } NMR (162 MHz, DMSO) δ -1.36 ppm.

Bis(2-ethylhexyl) hydrogen phosphate (2e): The product was obtained as colourless oil in 71% yield (230 mg, CAS No.: 298-07-7); ^1H NMR (400 MHz, Chloroform-*d*) δ 12.32 (s, 1H), 4.09 – 3.74 (m, 4H), 1.81 – 1.16 (m, 18H), 1.04 – 0.72 (m, 12H). ^{13}C { ^1H }

NMR (101 MHz, Chloroform-*d*) δ 69.4 (d, J = 6.2 Hz), 40 (d, J = 7.6 Hz), 29.8, 28.8, 23.1, 22.9, 14, 10.8 ppm; ^{31}P { ^1H } NMR (162 MHz, Chloroform-*d*) δ 1.08 ppm.

Diisopropyl hydrogen phosphate (2f) : The product was obtained as colourless oil in 77% yield (141mg, CAS No.: 1611-31-0); ^1H NMR (400 MHz, Chloroform-*d*) δ 11.02 (s, 1H), 4.62 (dp, J = 7.1, 6.2 Hz, 1H), 1.36 (dd, J = 6.2, 0.6 Hz, 7H). ^{13}C { ^1H } NMR (101 MHz, Chloroform-*d*) δ 72.3 (d, J = 5.9 Hz), 23.5 (d, J = 5.2 Hz) ppm; ^{31}P { ^1H } NMR (162 MHz, Chloroform-*d*) δ 0.07 ppm.

Bis-(2,2,2-trifluoroethyl) hydrogen phosphate (2h): The product was obtained as a colourless oil in 83% yield (217 mg, CAS No.: 92466-70-1); ^1H NMR (400 MHz, DMSO-*d*₆) δ 8.24 (s, 1H), 4.36 – 4.55 (m, 4H); ^{13}C { ^1H } (101 MHz, DMSO-*d*₆) δ 131.5 – 116.5 (m), 62.5 (q, J = 35.2 Hz) ppm; ^{31}P { ^1H } NMR (162 MHz, DMSO-*d*₆) δ -1.92.

Dibenzyl hydrogen phosphate (2i): The product was obtained as a yellow oil in 96% yield (225 mg, CAS No.: 1623-08-1); ^1H NMR (400 MHz, DMSO-*d*₆) δ 9.70 (s, 1H), 7.87 – 6.94 (m, 10H), 5.10 (d, J = 8.2 Hz, 0.6H), 5.03 (d, J = 7.6 Hz, 3.4H). ^{13}C { ^1H } (101 MHz, DMSO-*d*₆) δ 137.3 (d, J = 7.2 Hz), 136.5, 130.9 – 125.4 (m), 69.1 (d, J = 5.4 Hz), 68 (d, J = 5.4 Hz), 67.3 ppm; ^{31}P { ^1H } NMR (162 MHz, DMSO-*d*₆) δ -1.23, -1.01.

Diphenyl hydrogen phosphate (2j): The product was obtained as a white solid in 90% yield (225 mg, CAS No.: 838-85-7); ^1H NMR (400 MHz, DMSO-*d*₆) δ 7.40 (m, J = 9.7, 5.8, 2.2 Hz, 5H), 7.26 – 7.12 (m, 6H); ^{13}C { ^1H } NMR (101 MHz, DMSO-*d*₆) δ 151.6 (d, J = 6.9 Hz), 130.2, 124.9, 120.4 (d, J = 5.1 Hz) ppm; ^{31}P { ^1H } NMR (162 MHz, DMSO-*d*₆) δ -12.15 ppm.

Diphenylphosphinic acid (2k): The product was obtained as a colourless oil 99% yield (218 mg, CAS No.: 1707-03-5); ^1H NMR (400 MHz, $\text{DMSO-}d_6$) δ 10.88 (s, 1H), 7.75 (m, 4H), 7.64 – 7.34 (m, 6H); $^{13}\text{C}\{^1\text{H}\}$ NMR (101 MHz, $\text{DMSO-}d_6$) δ 135.5 (d, $J = 135.1$ Hz), 131.9, 131.4 (d, $J = 9.8$ Hz), 128.9 (d, $J = 12.4$ Hz) ppm; $^{31}\text{P}\{^1\text{H}\}$ NMR (162 MHz, $\text{DMSO-}d_6$) δ 23.23 ppm.

Bis-(4-chlorodiphenyl)phosphinic acid (2l): The product was obtained as a red solid 92% yield (264 mg, CAS No.: 13119-01-2); ^1H NMR (400 MHz, $\text{DMSO-}d_6$) δ 7.83 – 7.70 (m, 4H), 7.58 (dq, $J = 8.8, 2.3$ Hz, 4H), 6.27 (s, 1H). $^{13}\text{C}\{^1\text{H}\}$ NMR (101 MHz, $\text{DMSO-}d_6$) δ 137.2, 134.8, 133.3 (d, $J = 11.2$ Hz), 129.1 (d, $J = 13.2$ Hz) ppm; $^{31}\text{P}\{^1\text{H}\}$ NMR (162 MHz, $\text{DMSO-}d_6$) δ 21.2 ppm.

Bis-(4-Methoxydiphenyl)phosphinic acid (2m): The product was obtained as white solid 89% yield (247 mg, CAS No.: 20434-05-3); ^1H NMR (400 MHz, $\text{DMSO-}d_6$) δ 7.67 (dtd, $J = 13.2, 6.4, 2.7$ Hz, 4H), 7.08 – 6.98 (m, 4H), 5.40 (s, 1H), 3.81 (s, 6H). $^{13}\text{C}\{^1\text{H}\}$ NMR (101 MHz, $\text{DMSO-}d_6$) δ 161.9, 133.2 (d, $J = 11.2$ Hz), 127.3 (d, $J = 141.9$ Hz), 114.3 (d, $J = 13.5$ Hz), 55.7 ppm; $^{31}\text{P}\{^1\text{H}\}$ NMR (162 MHz, $\text{DMSO-}d_6$) δ 23.98 ppm.

bis(4-(trifluoromethyl)phenyl)phosphinic acid (2n): The product was obtained as brown solid 86% yield (304 mg, CAS No.: 1869-27-8); ^1H NMR (400 MHz, DMSO) δ 8.00 (dd, $J = 11.6, 7.9$ Hz, 4H), 7.87 (dd, $J = 8.3, 2.6$ Hz, 4H), 5.21 (s, 1H); $^{13}\text{C}\{^1\text{H}\}$ (101 MHz, $\text{DMSO-}d_6$) δ 139.5 (d, $J = 132.9$ Hz), 132.4 (d, $J = 10.5$ Hz), 125.9 (d, $J = 12.4$ Hz); $^{31}\text{P}\{^1\text{H}\}$ NMR (162 MHz, $\text{DMSO-}d_6$) δ 19.77.

((2-chlorophenyl)(hydroxy)methyl)phosphonic acid (4): The product was obtained as white solid 95% yield (222 mg, CAS No.: 20641-28-5); ^1H NMR (400 MHz, DMSO) δ 8.76 (s, 5H), 7.71 (dt, $J = 7.8, 2.1$ Hz, 1H), 7.44 – 7.34 (m, 2H), 7.30 (tt, $J = 7.5, 1.8$ Hz, 1H), 5.17 (d, $J = 14.1$ Hz, 1H); $^{13}\text{C}\{^1\text{H}\}$ (101 MHz, $\text{DMSO-}d_6$) δ 138.5, 132.6, 130.6, 129, 127.1, 66.8 (d, $J = 161.6$ Hz); $^{31}\text{P}\{^1\text{H}\}$ NMR (162 MHz, $\text{DMSO-}d_6$) δ 17.85.

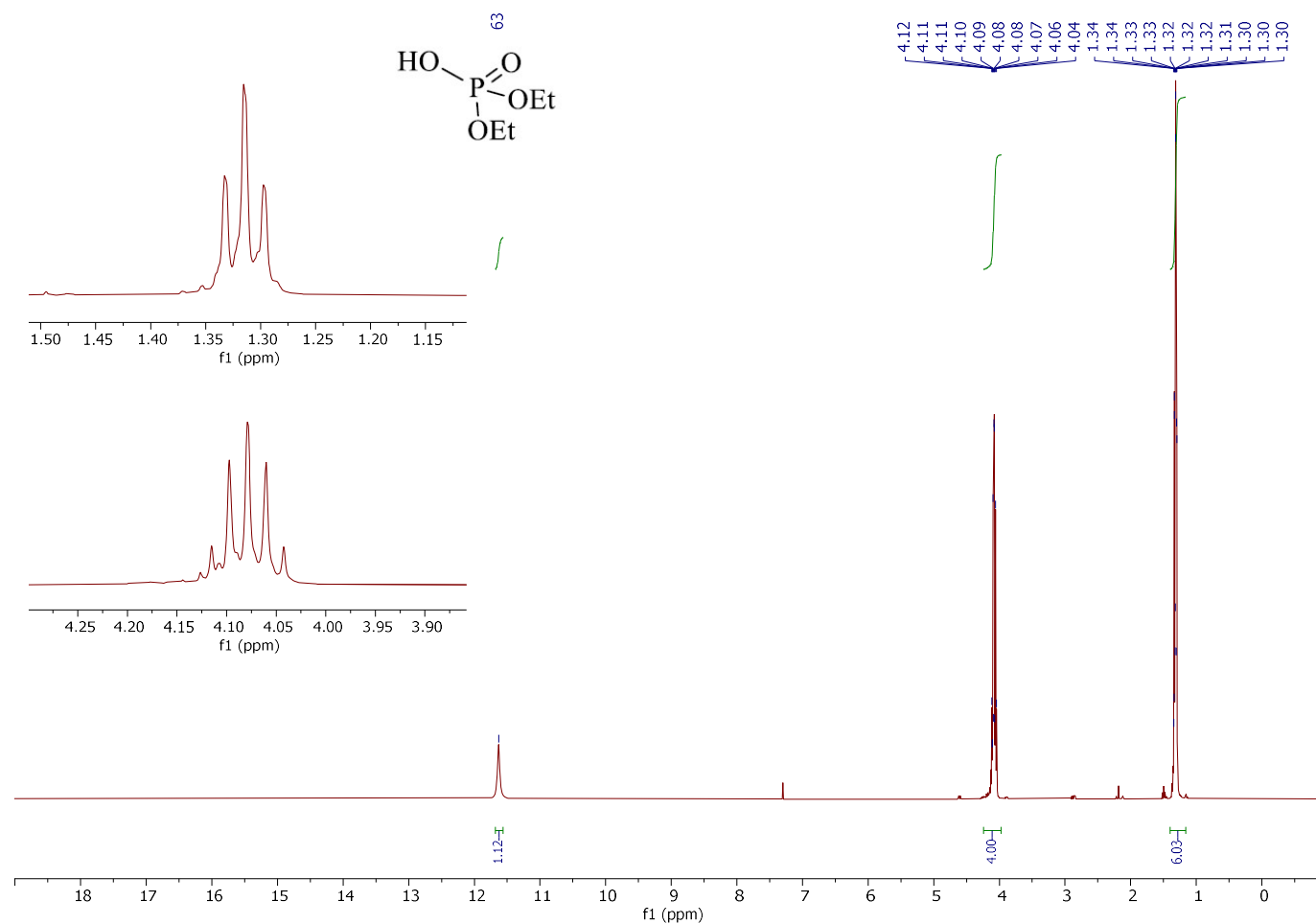


Figure S1: ^1H NMR Spectra of 2a in CDCl_3

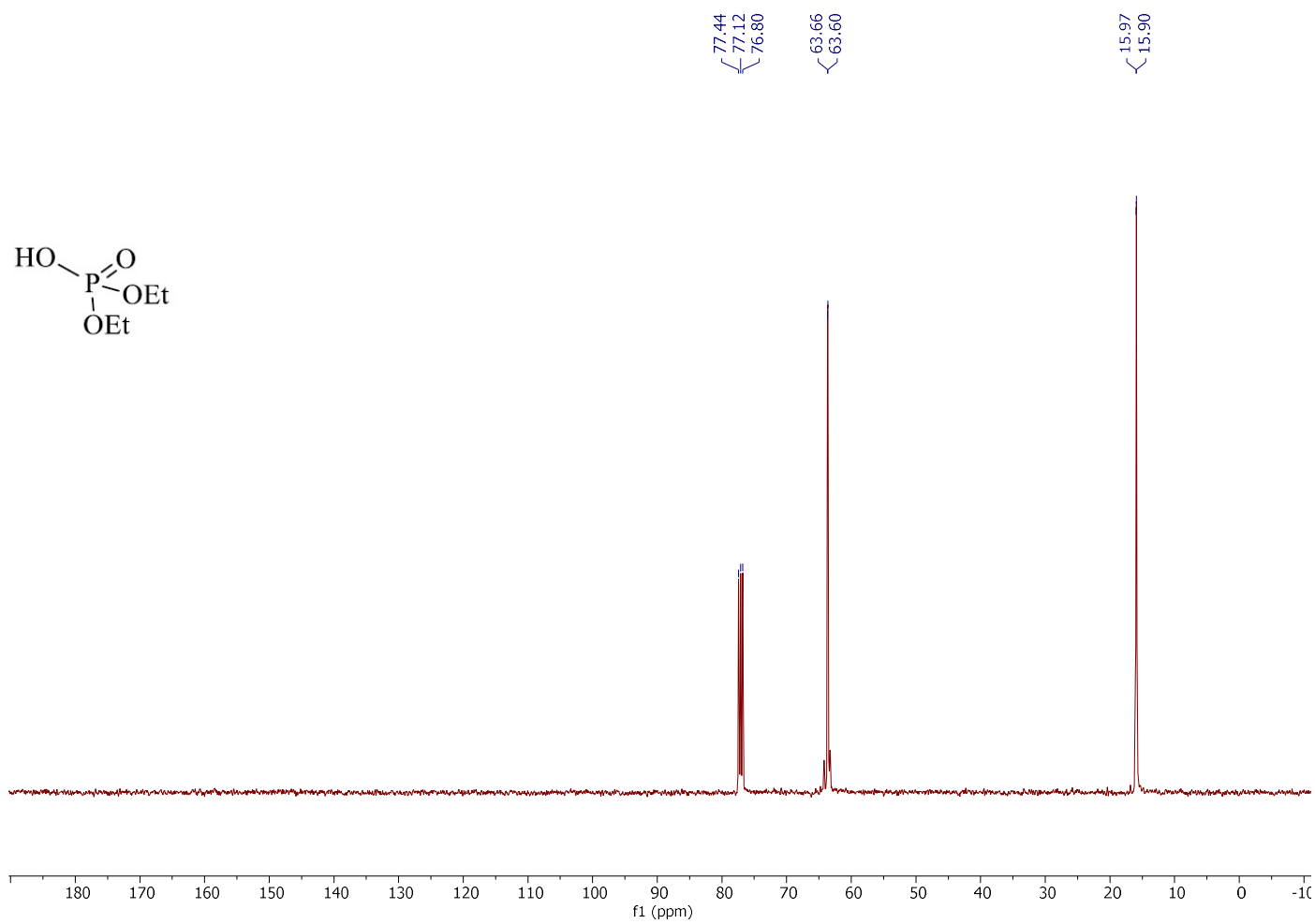


Figure S2: ^{13}C NMR Spectra of 2a in CDCl_3

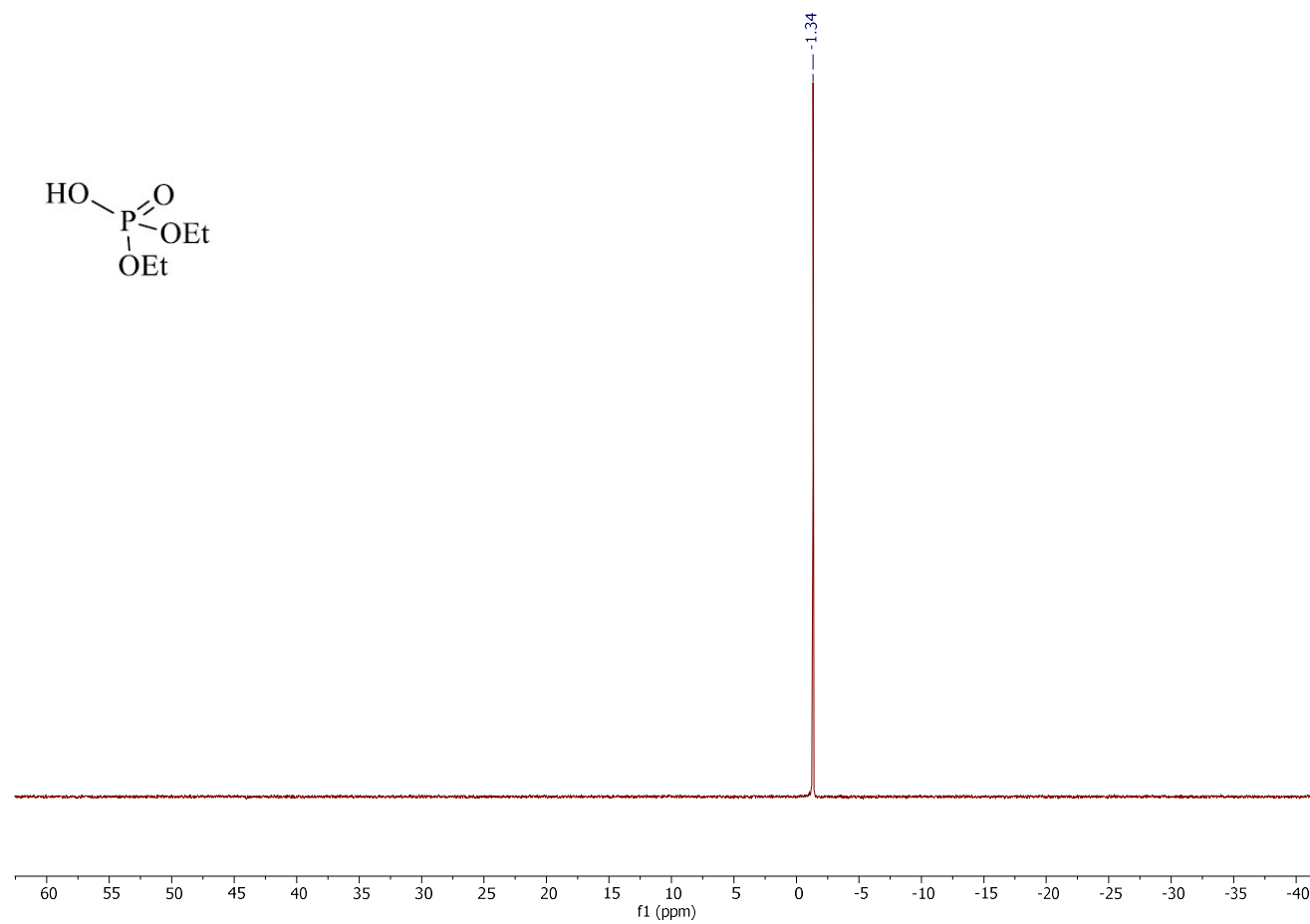


Figure S3: ^{31}P NMR Spectra of 2a in CDCl_3

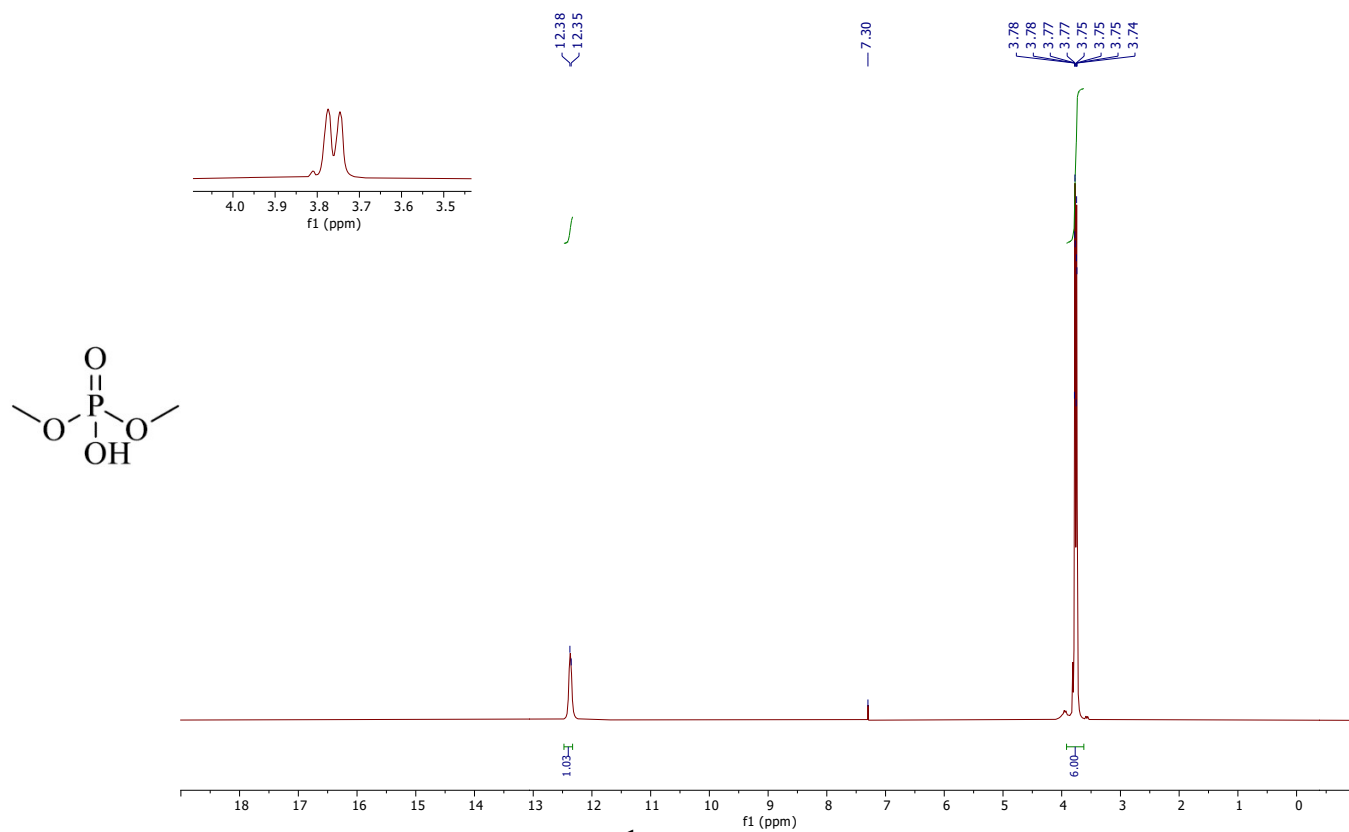


Figure S4: ^1H NMR Spectra of 2b in CDCl_3

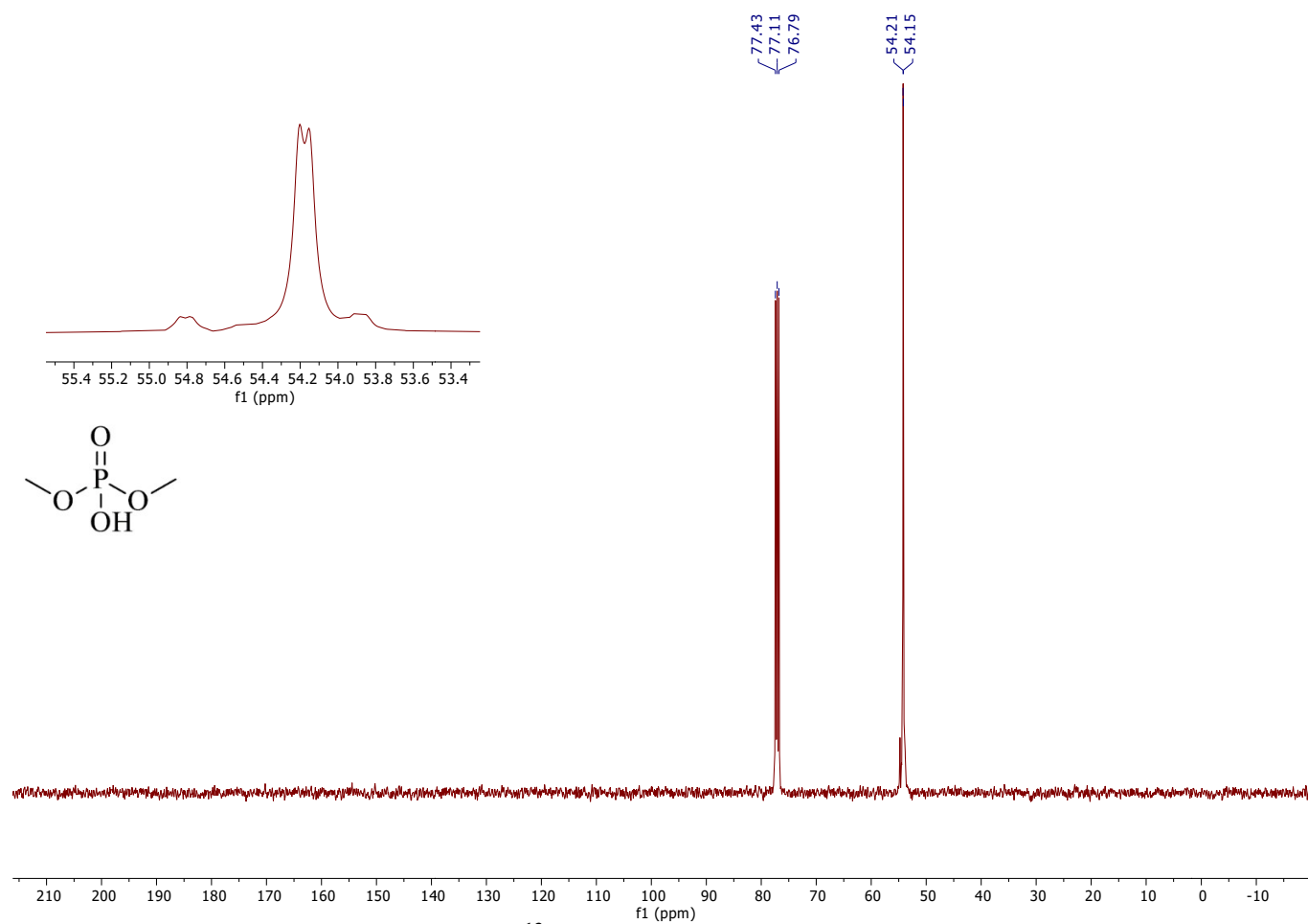


Figure S5: ^{13}C NMR Spectra of 2b in CDCl_3

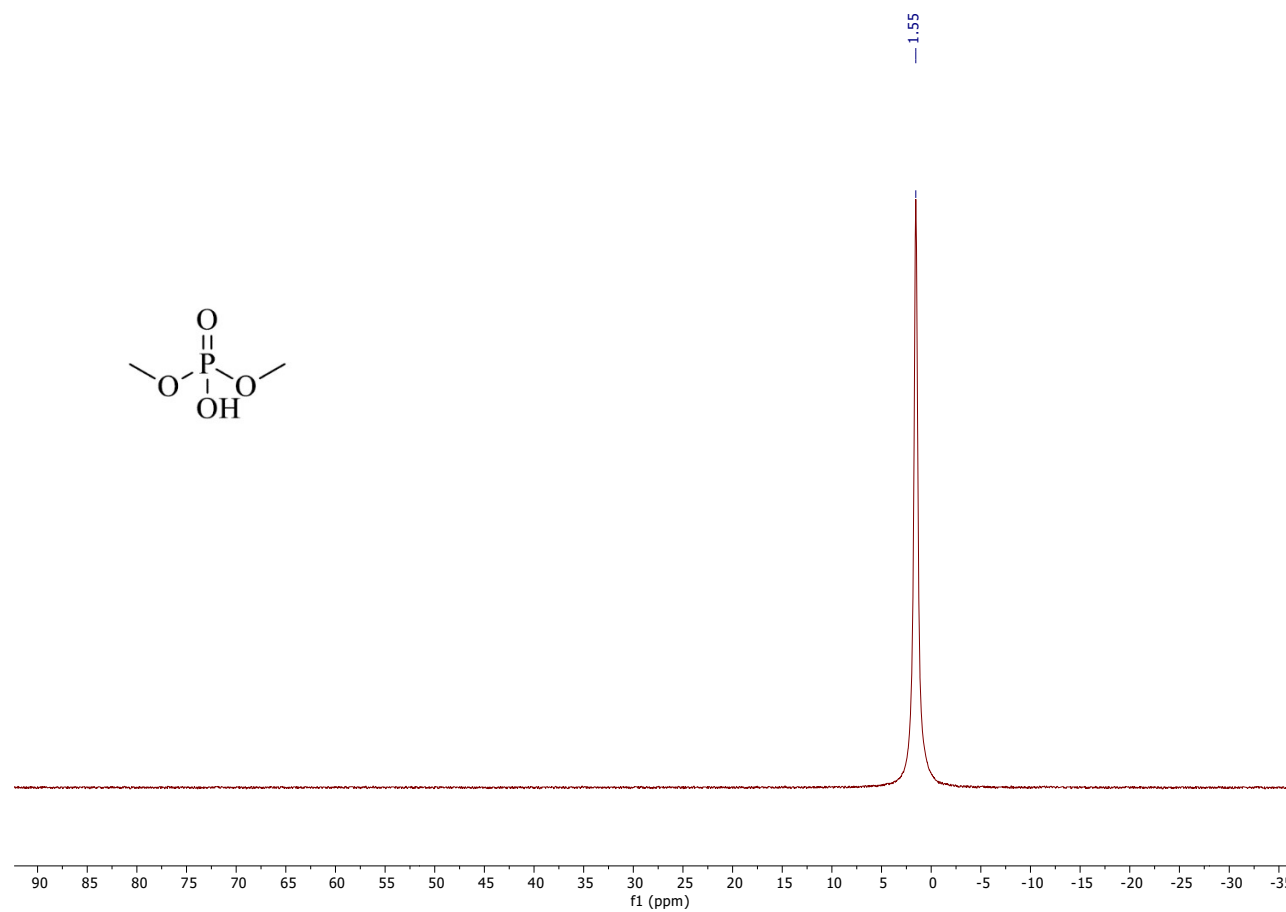


Figure S6: ^{31}P NMR Spectra of 2b in CDCl_3

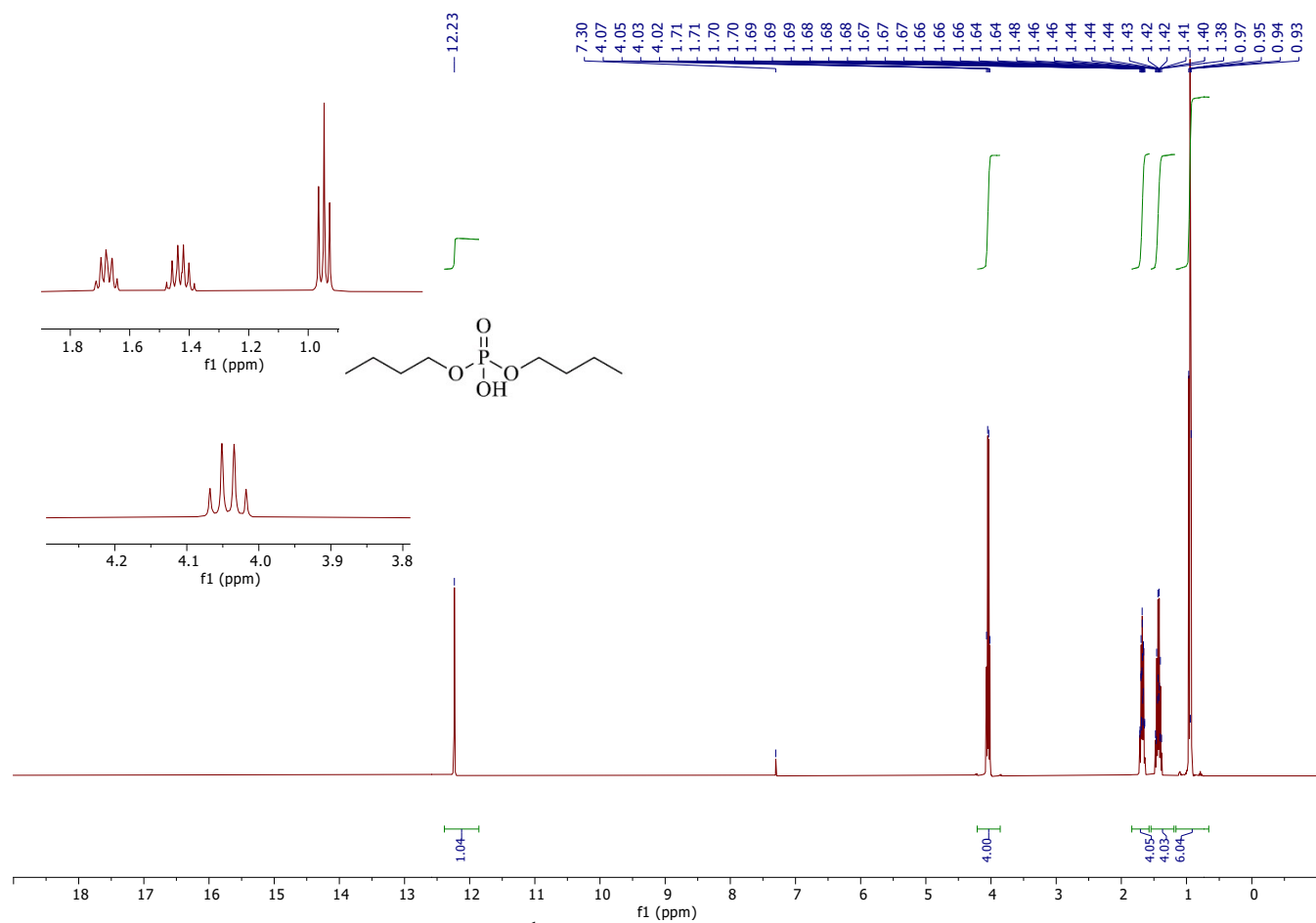


Figure S7: ^1H NMR Spectra of 2c in CDCl_3

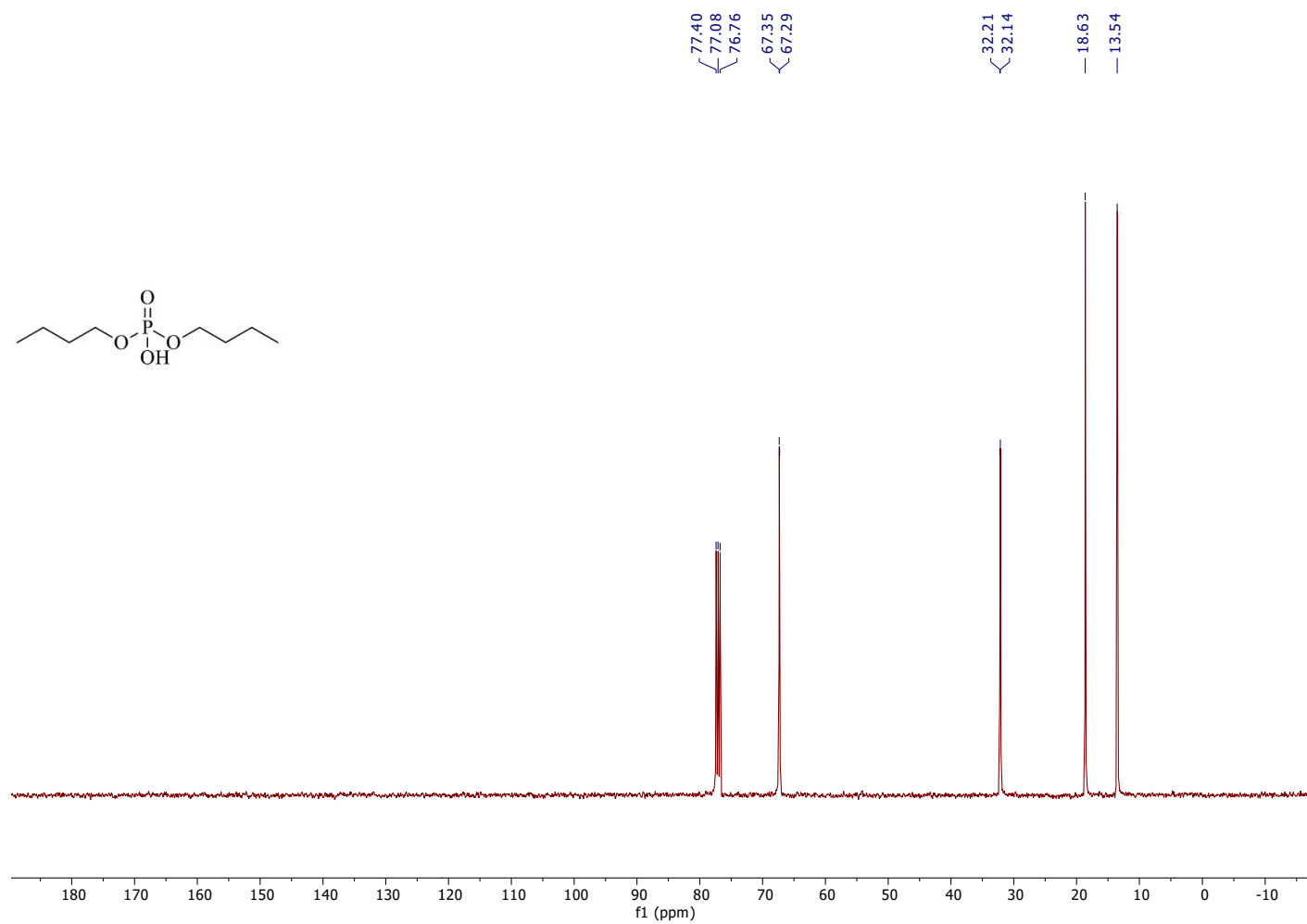


Figure S8: ^{13}C NMR Spectra of 2c in CDCl_3

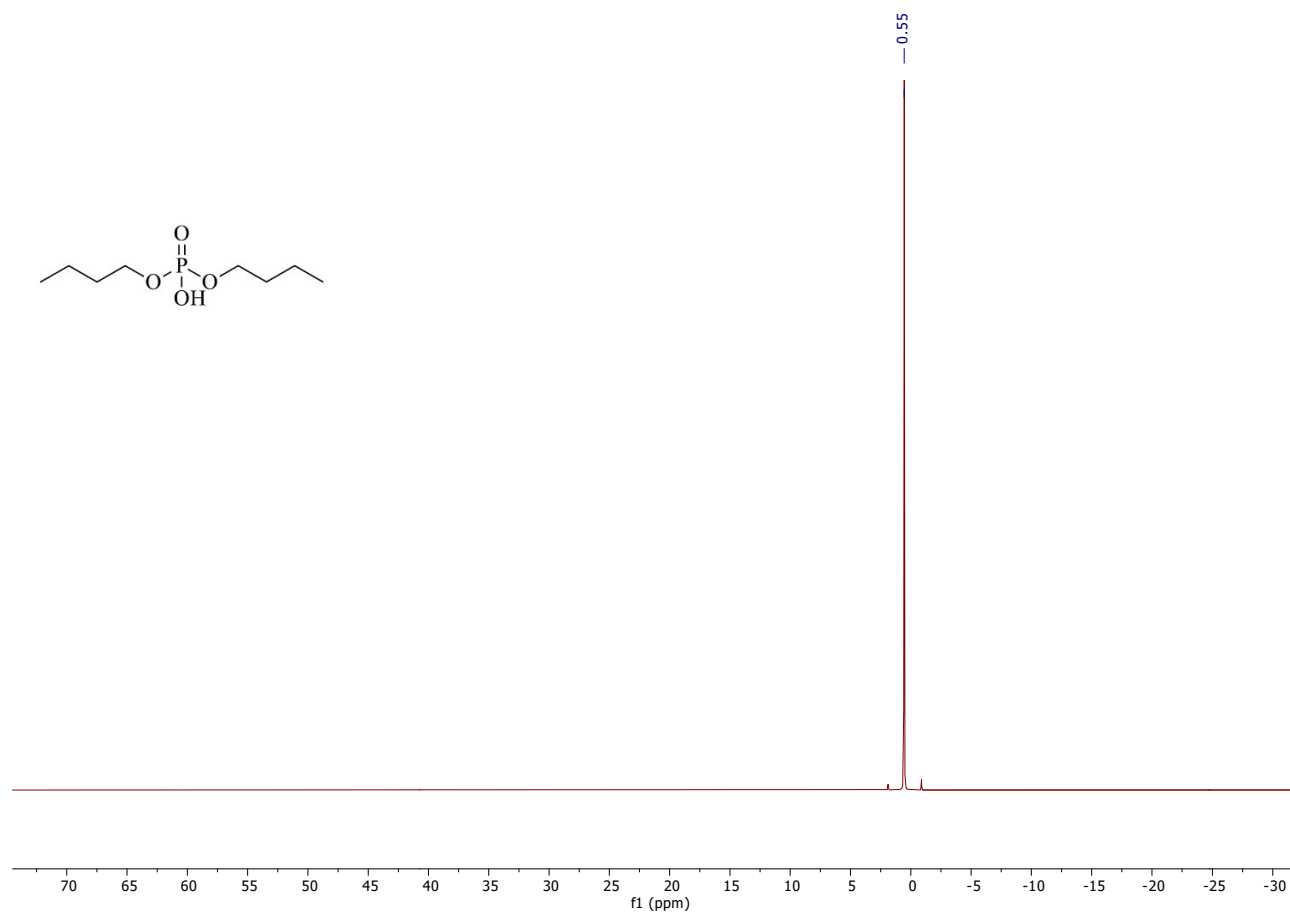


Figure S9: ³¹P NMR Spectra of 2c in CDCl₃

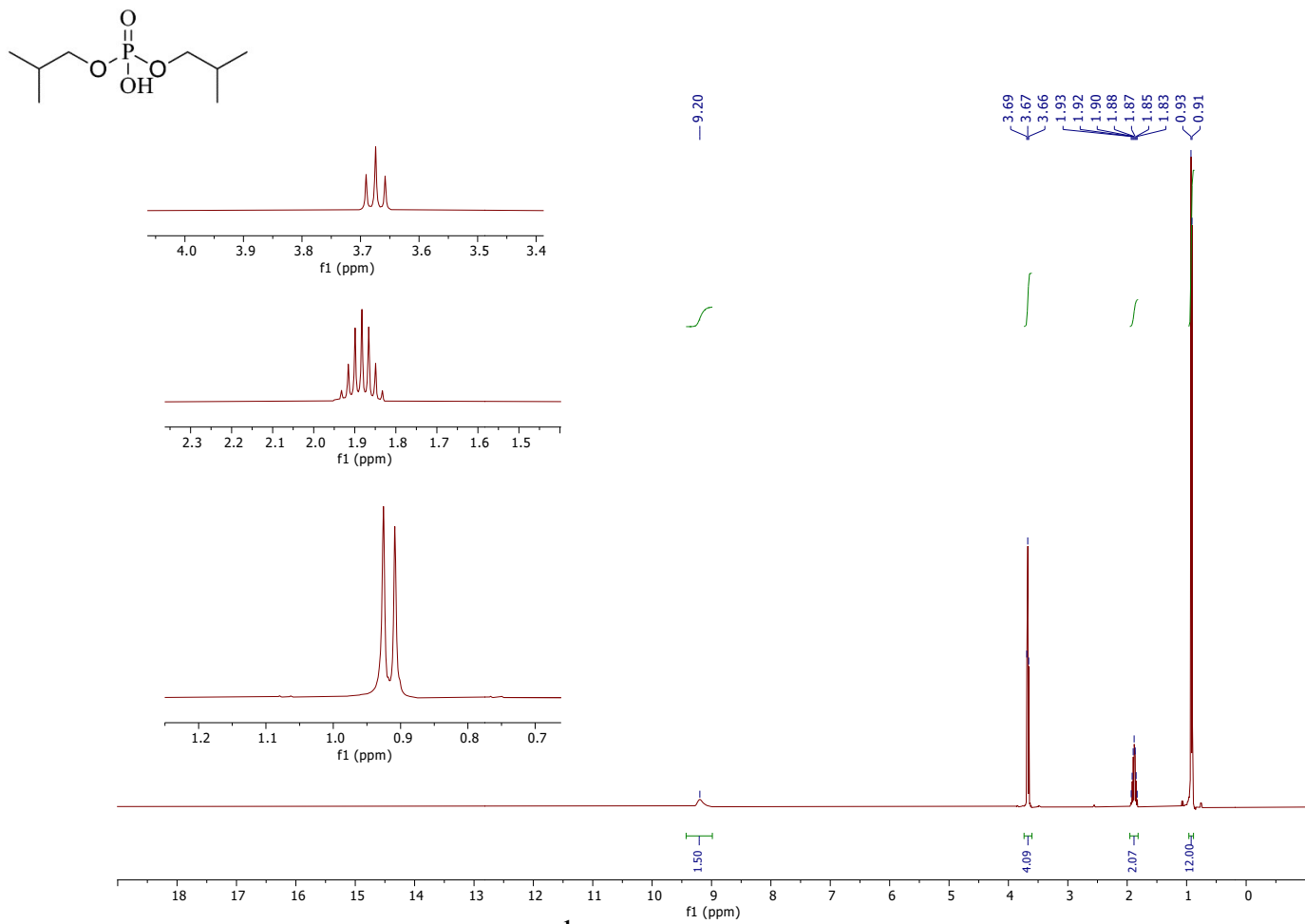


Figure S10: ^1H NMR Spectra of 2d in DMSO-d_6

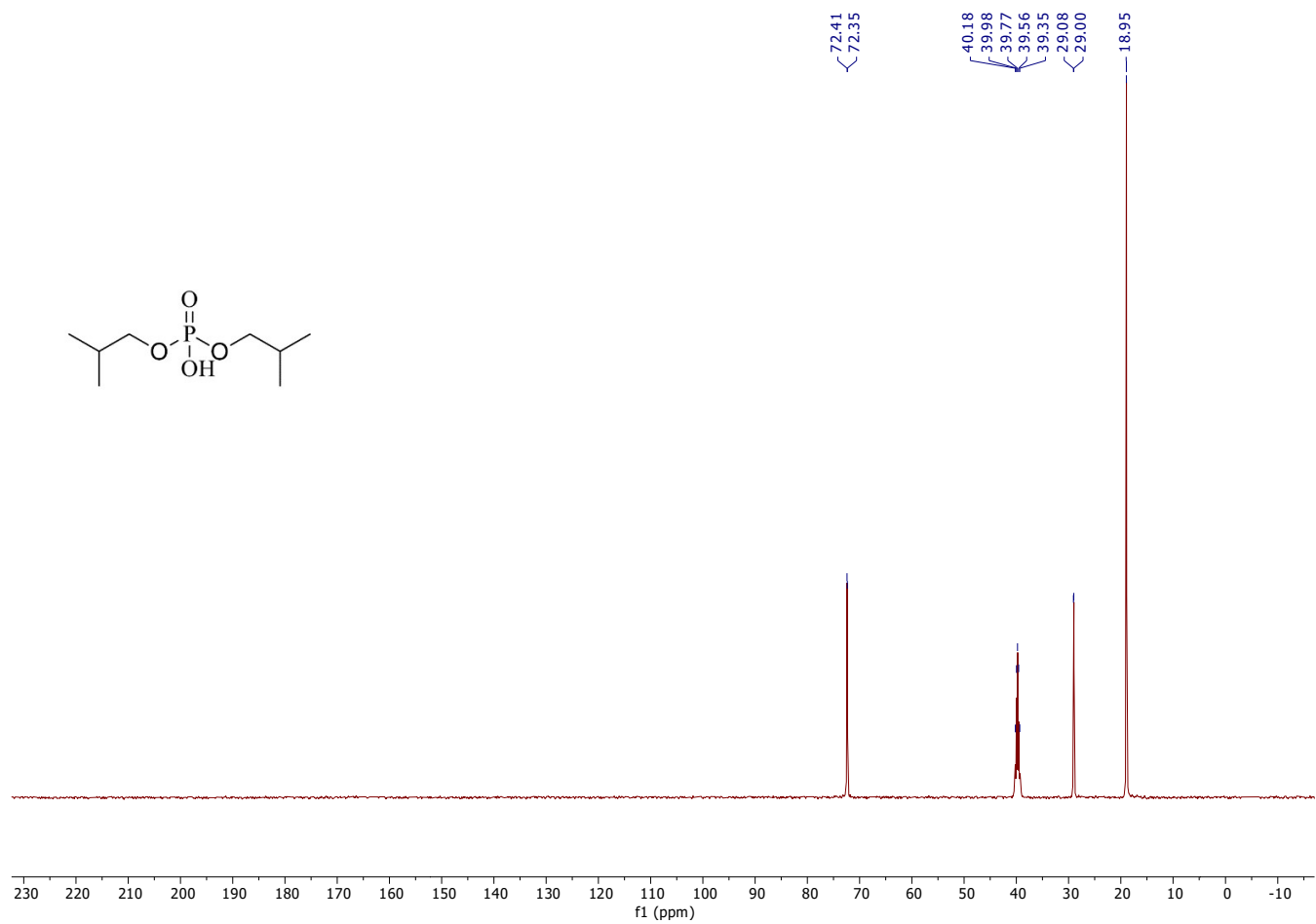


Figure S11: ¹³C NMR Spectra of 2d in DMSO-d₆

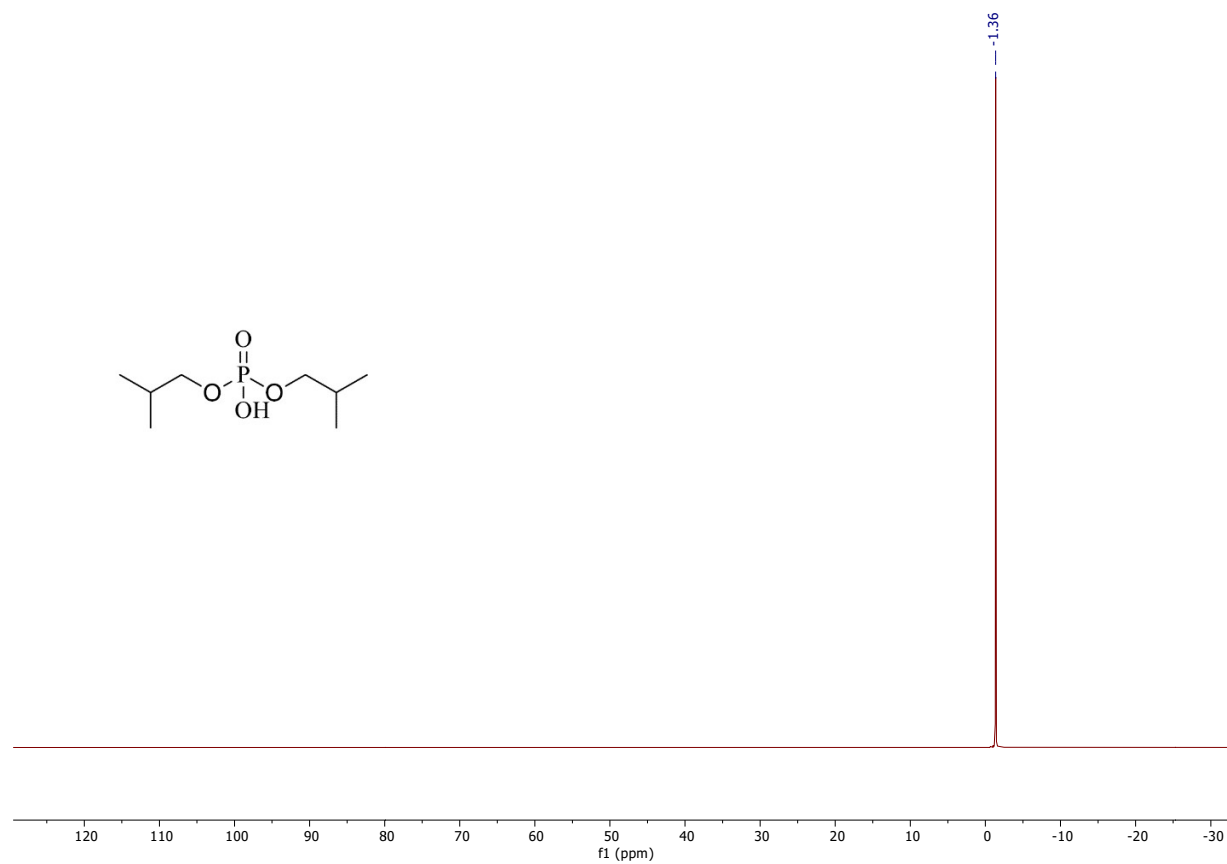


Figure S12: ^{31}P NMR Spectra of 2d in DMSO-d_6

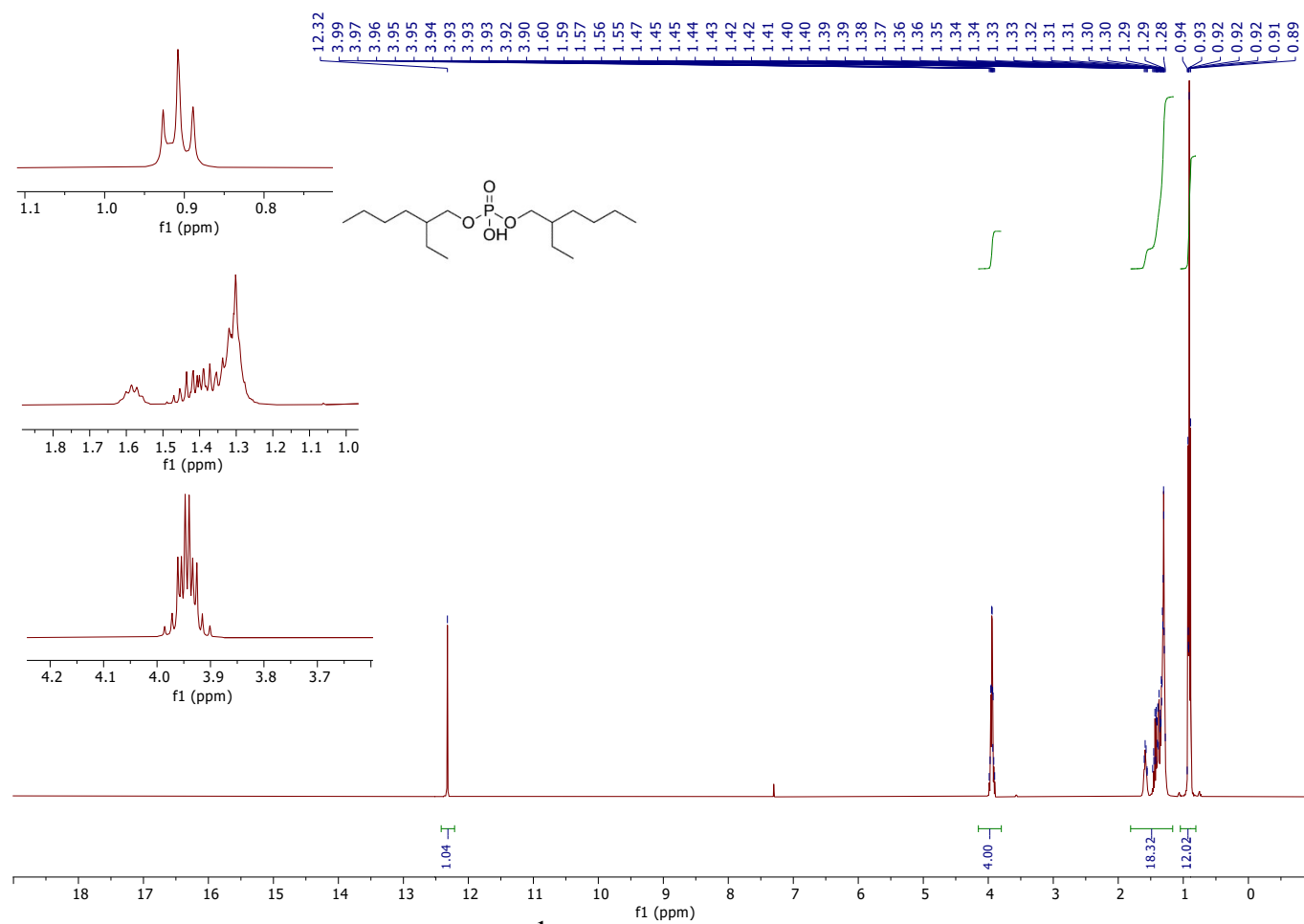


Figure S13: ^1H NMR Spectra of 2e in CDCl_3

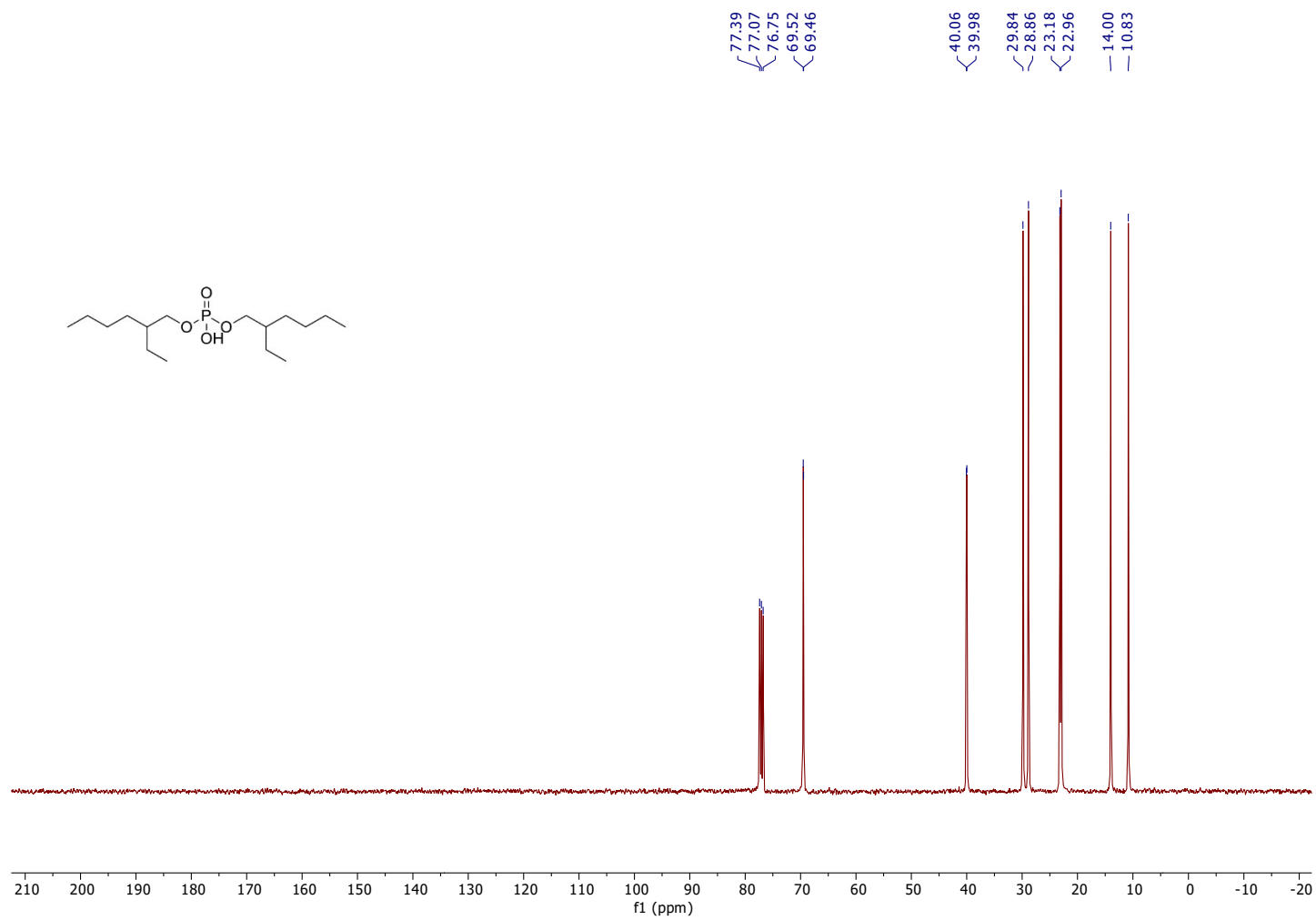


Figure S14: ^{13}C NMR Spectra of 2e in CDCl_3

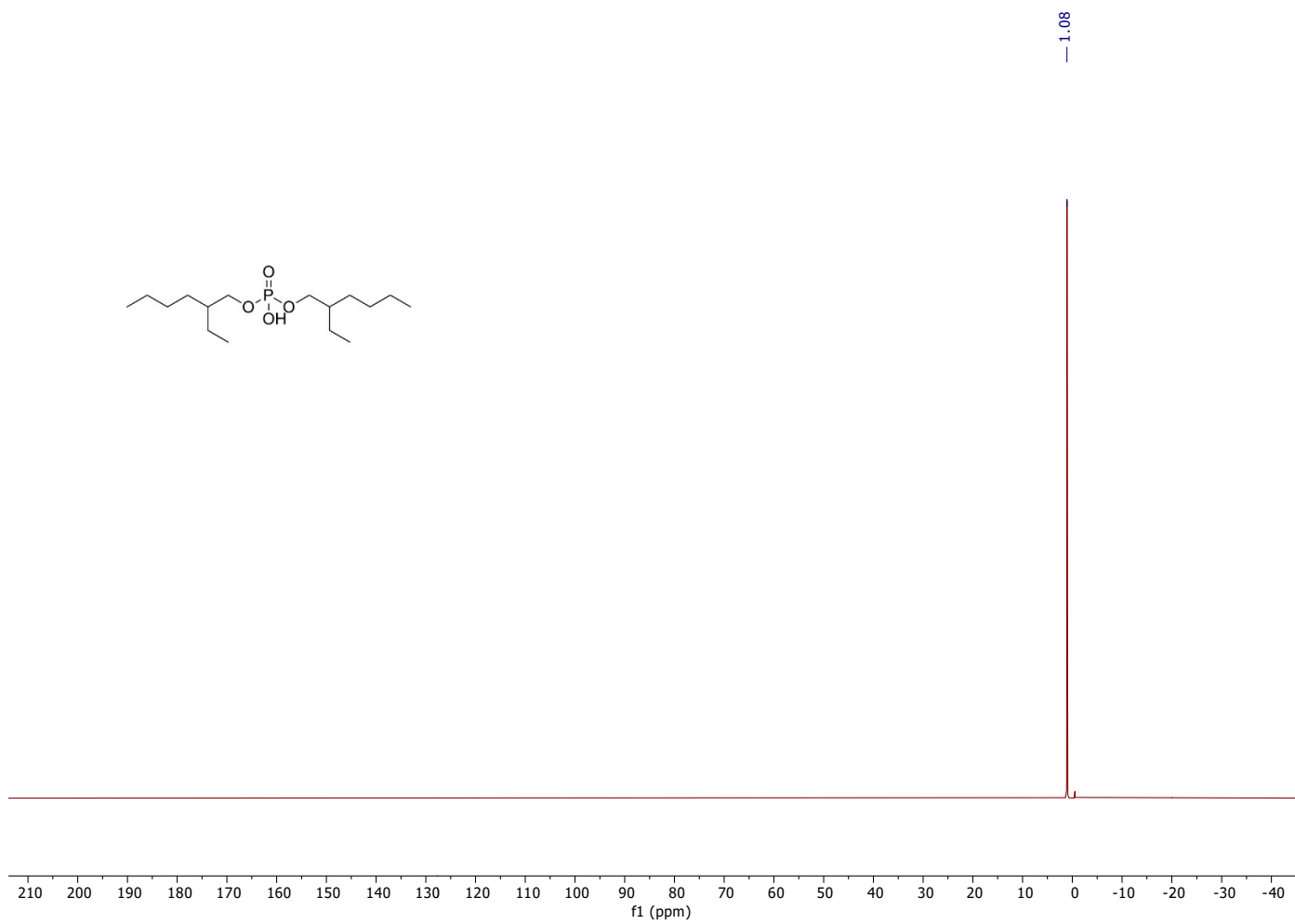


Figure S15: ^{31}P NMR Spectra of 2e in CDCl_3

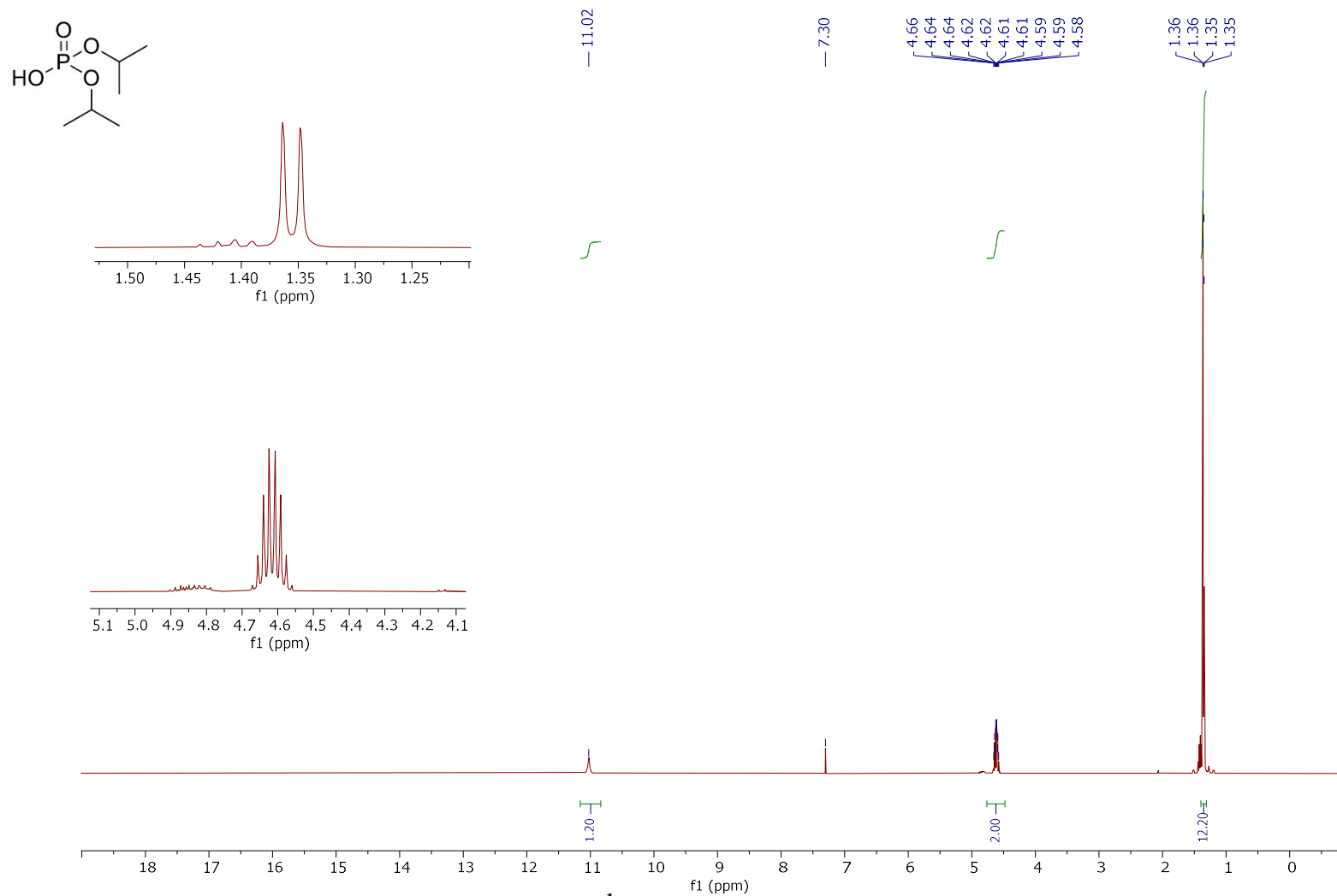


Figure S16: ^1H NMR Spectra of 2f in CDCl_3

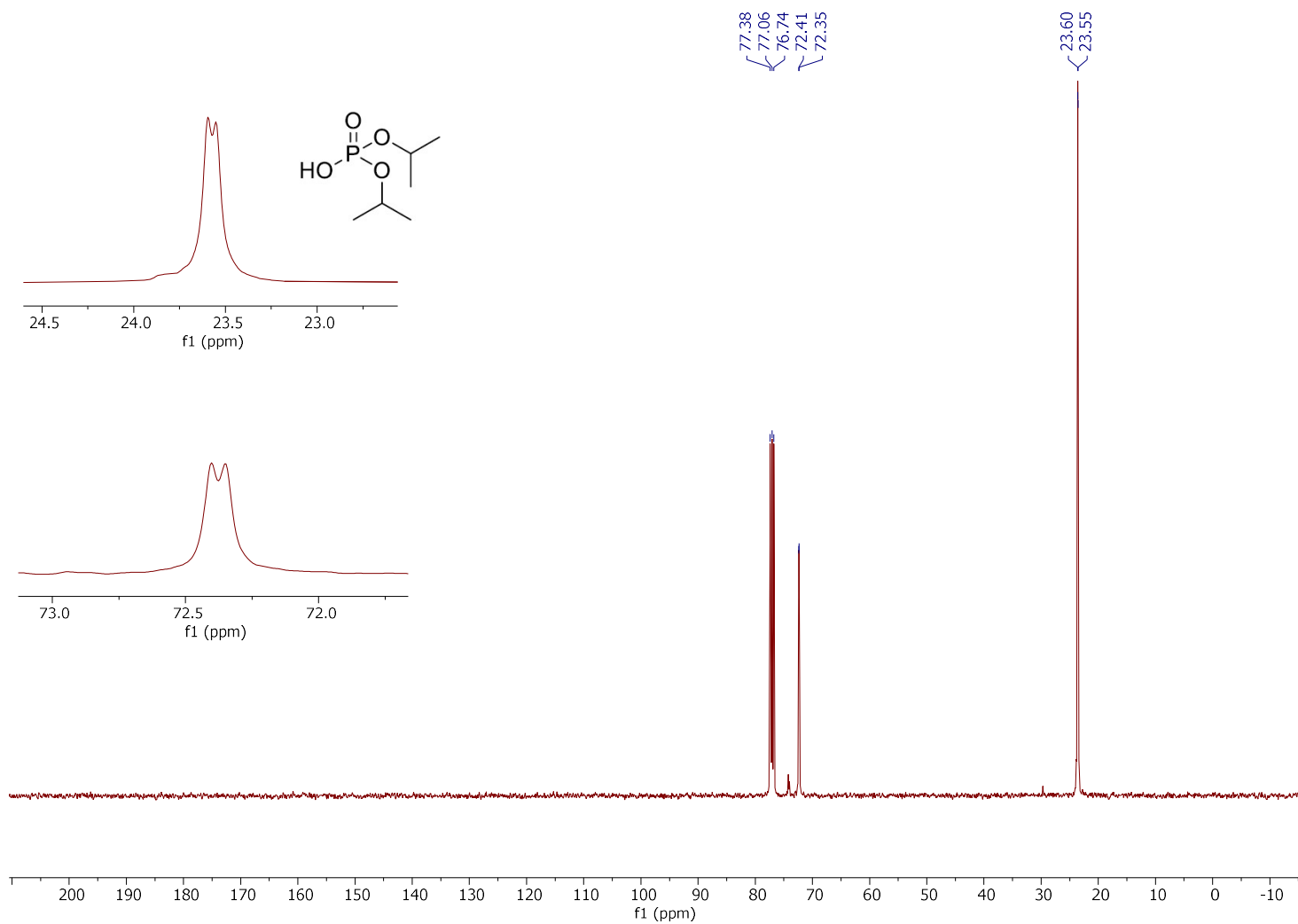


Figure S17: ^{13}C NMR Spectra of 2f in CDCl_3

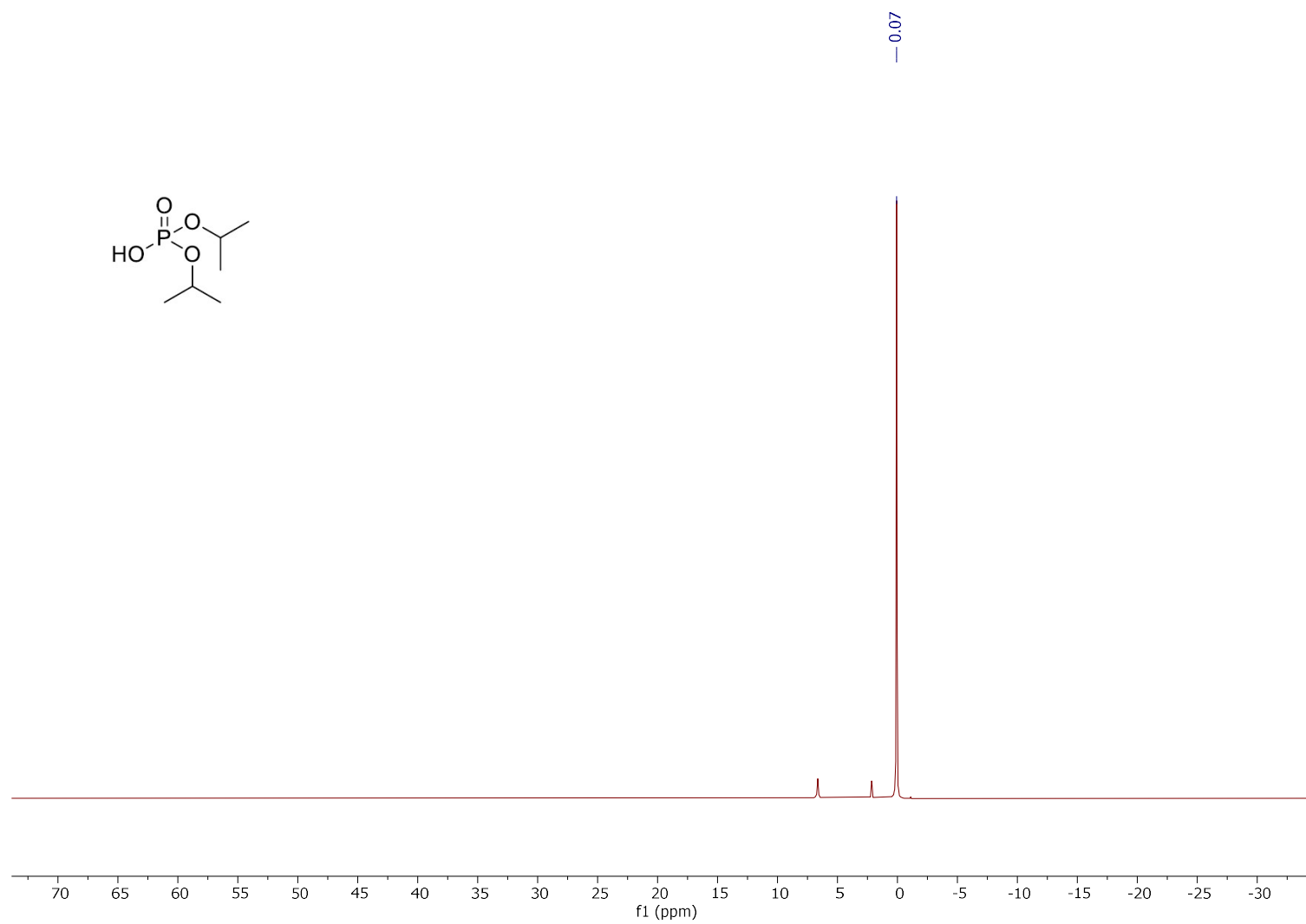


Figure S18: ^{31}P NMR Spectra of **2f** in CDCl_3

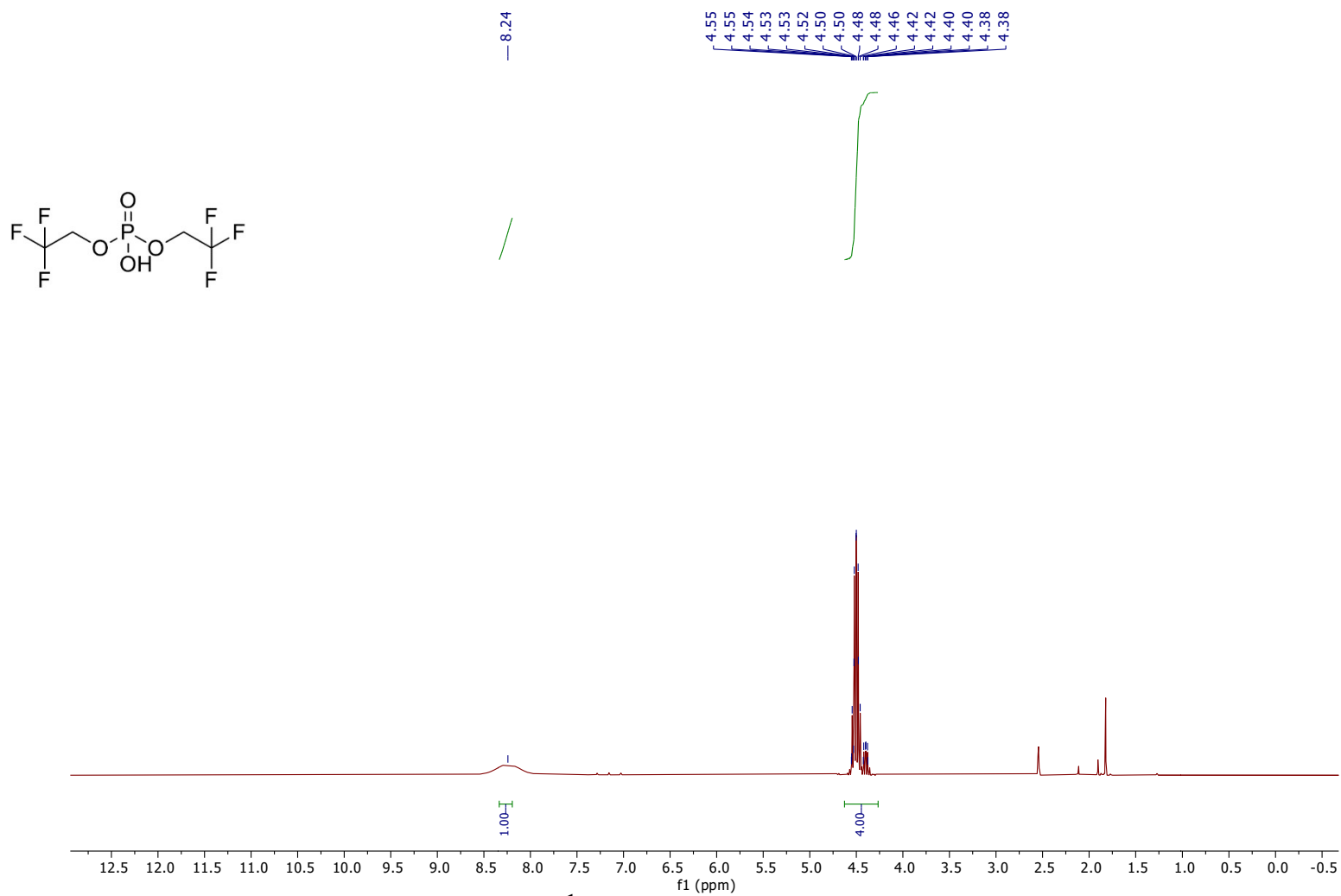


Figure S19: ¹H NMR Spectra of 2h in DMSO-d₆

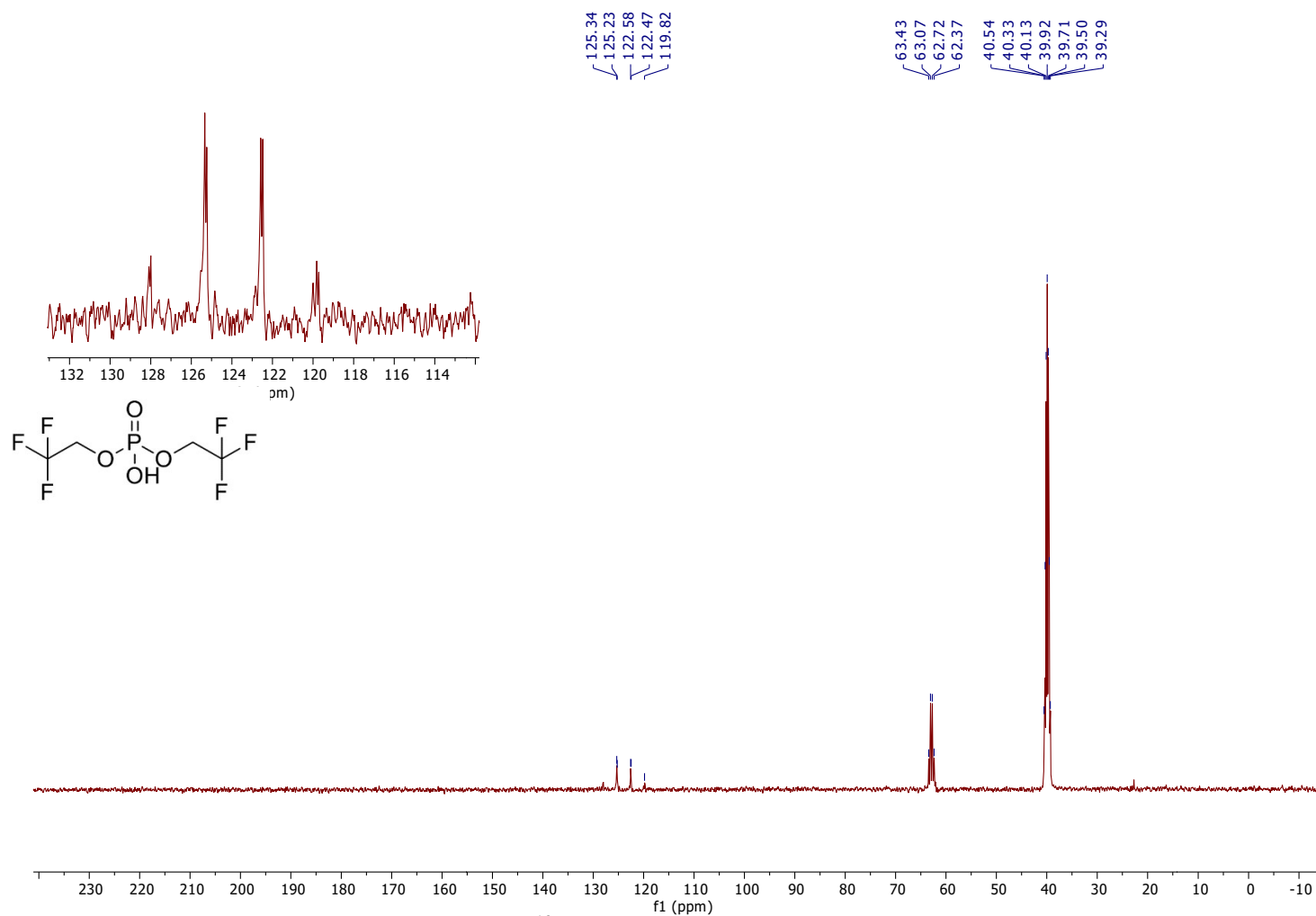


Figure S20: ^{13}C NMR Spectra of **2h** in DMSO-d_6

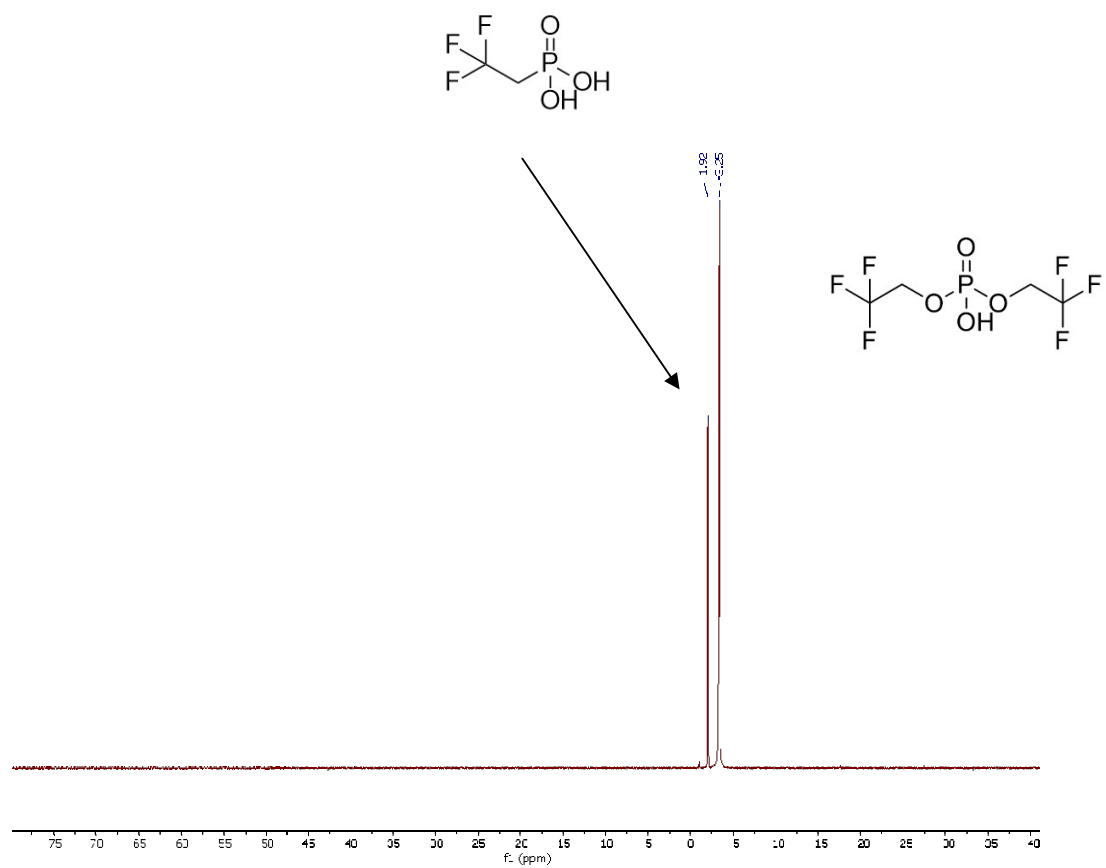


Figure S21: ^{31}P NMR Spectra of 2h in DMSO- d_6

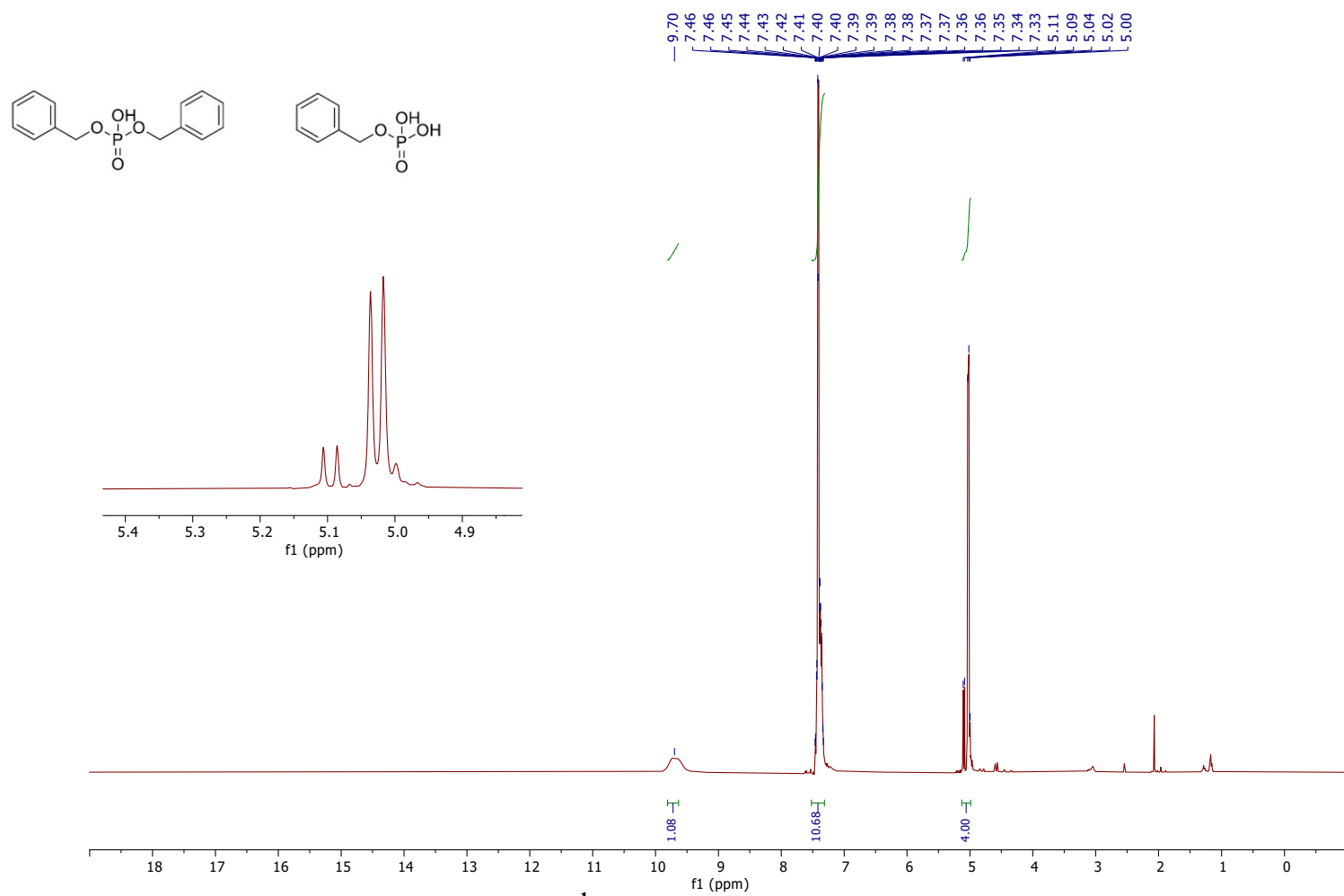


Figure S22: ^1H NMR Spectra of 2i in DMSO- d_6

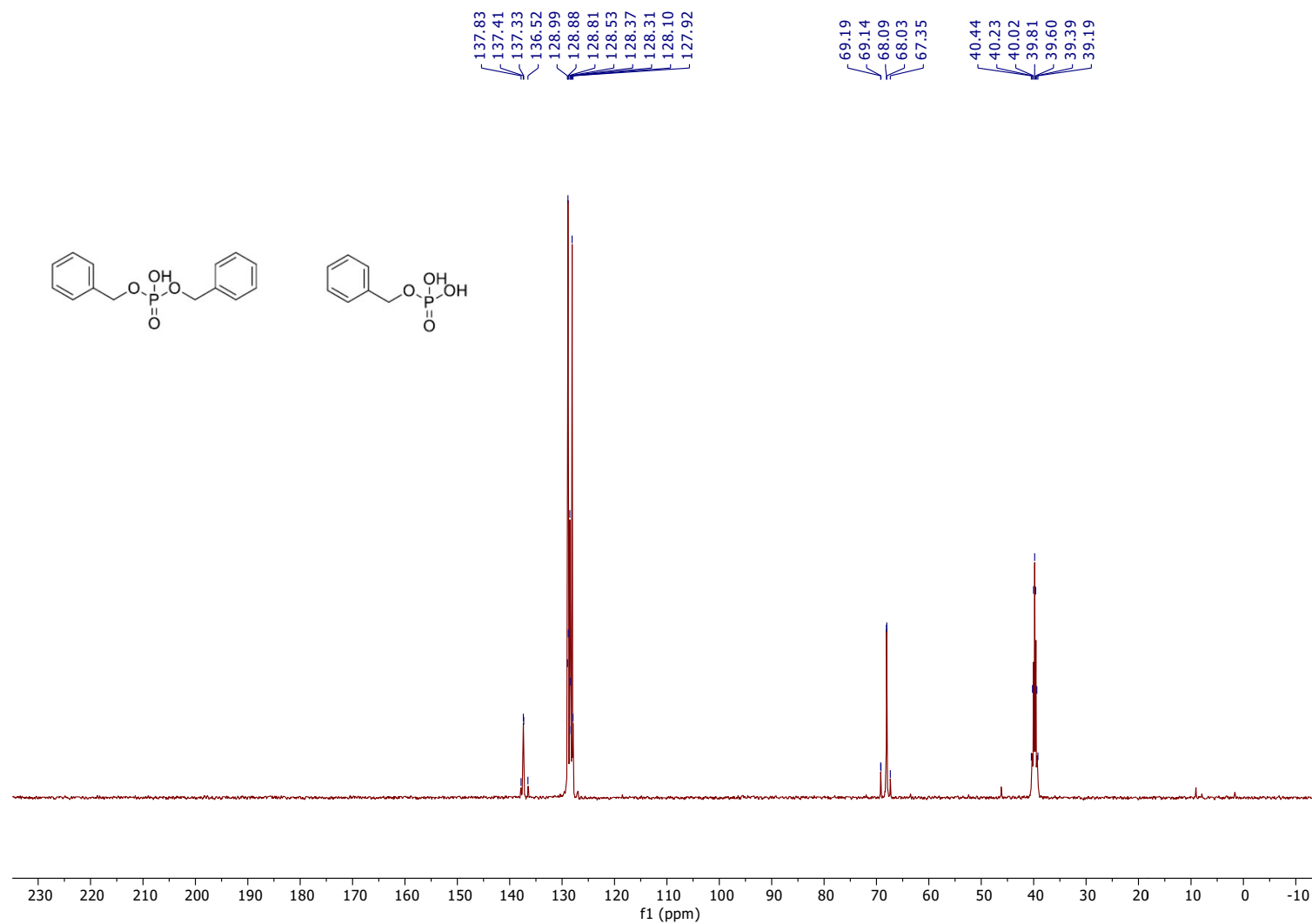


Figure S23: ^{13}C NMR Spectra of 2i in DMSO- d_6

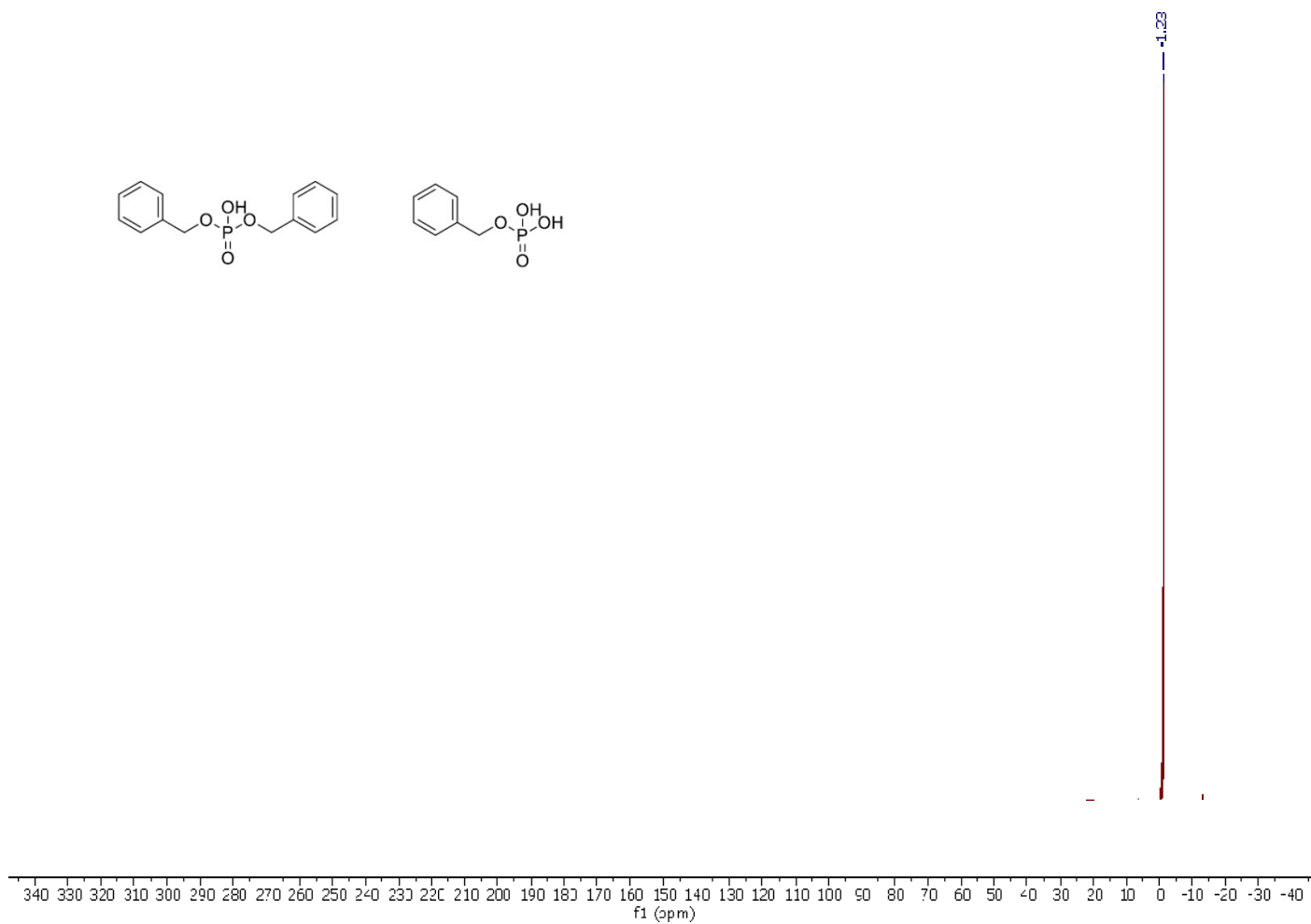


Figure S24: ^{31}P NMR Spectra of 2i in DMSO- d_6

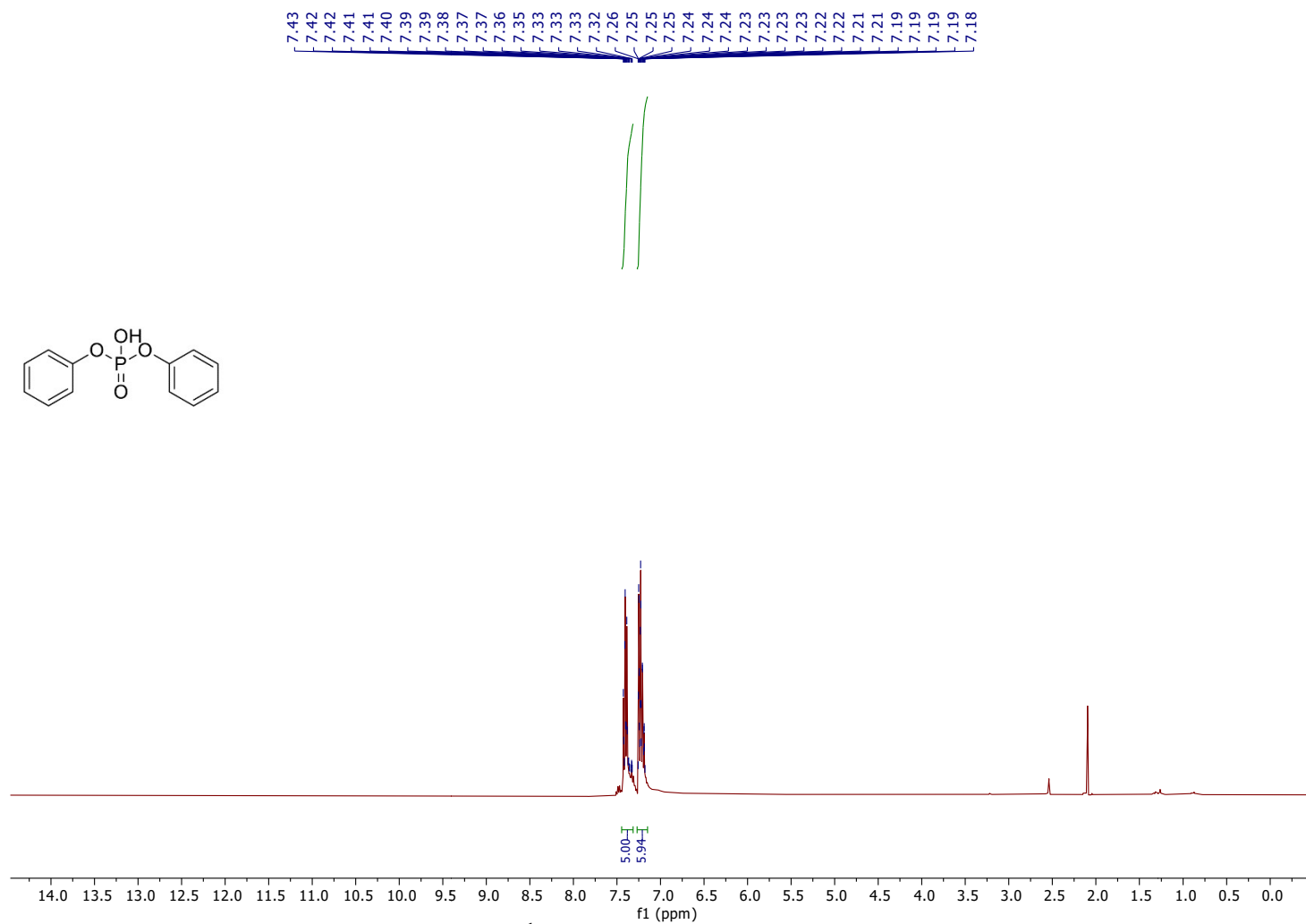


Figure S25: ¹H NMR Spectra of 2j in DMSO-d₆

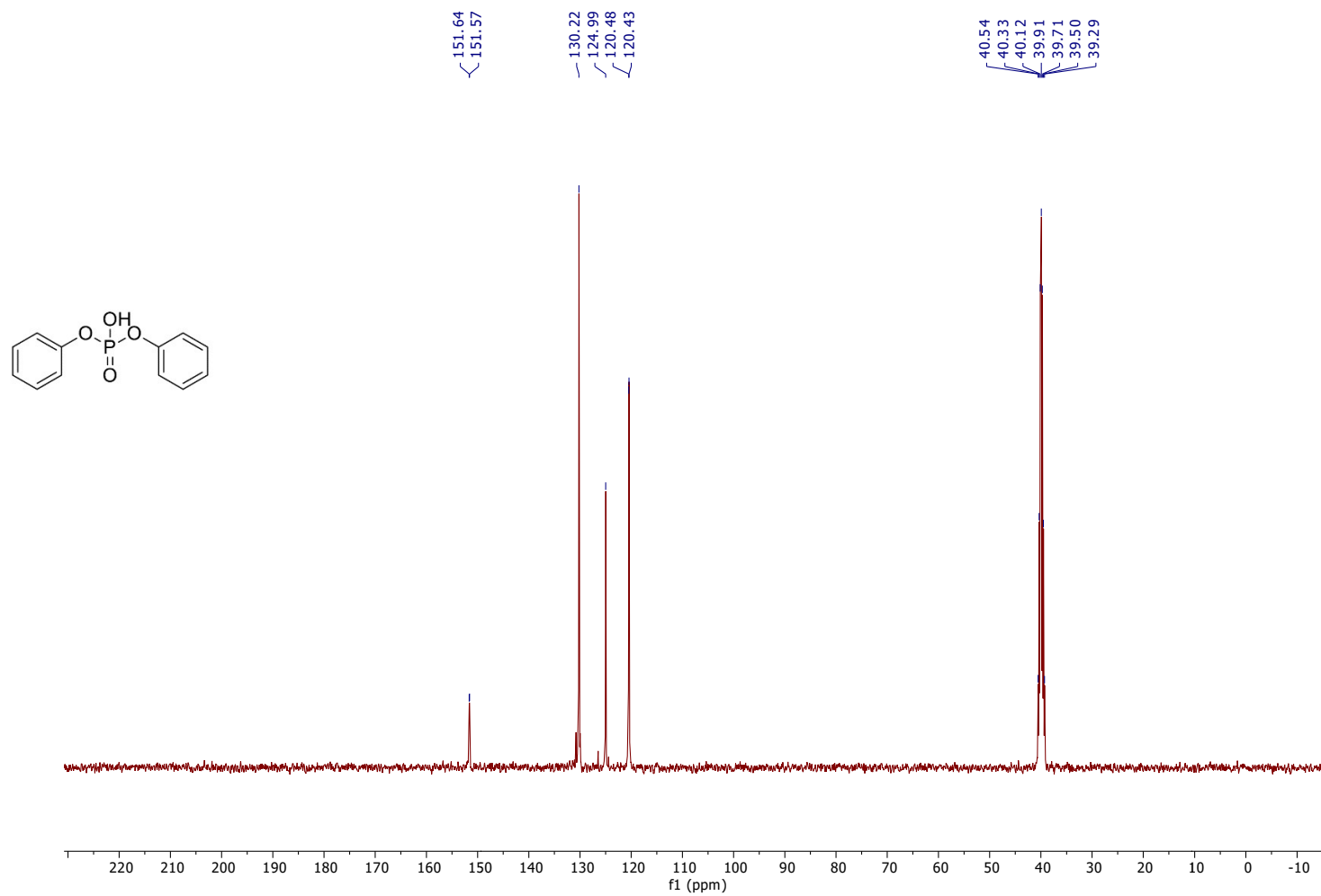


Figure S26: ¹³C NMR Spectra of 2j in DMSO-d₆

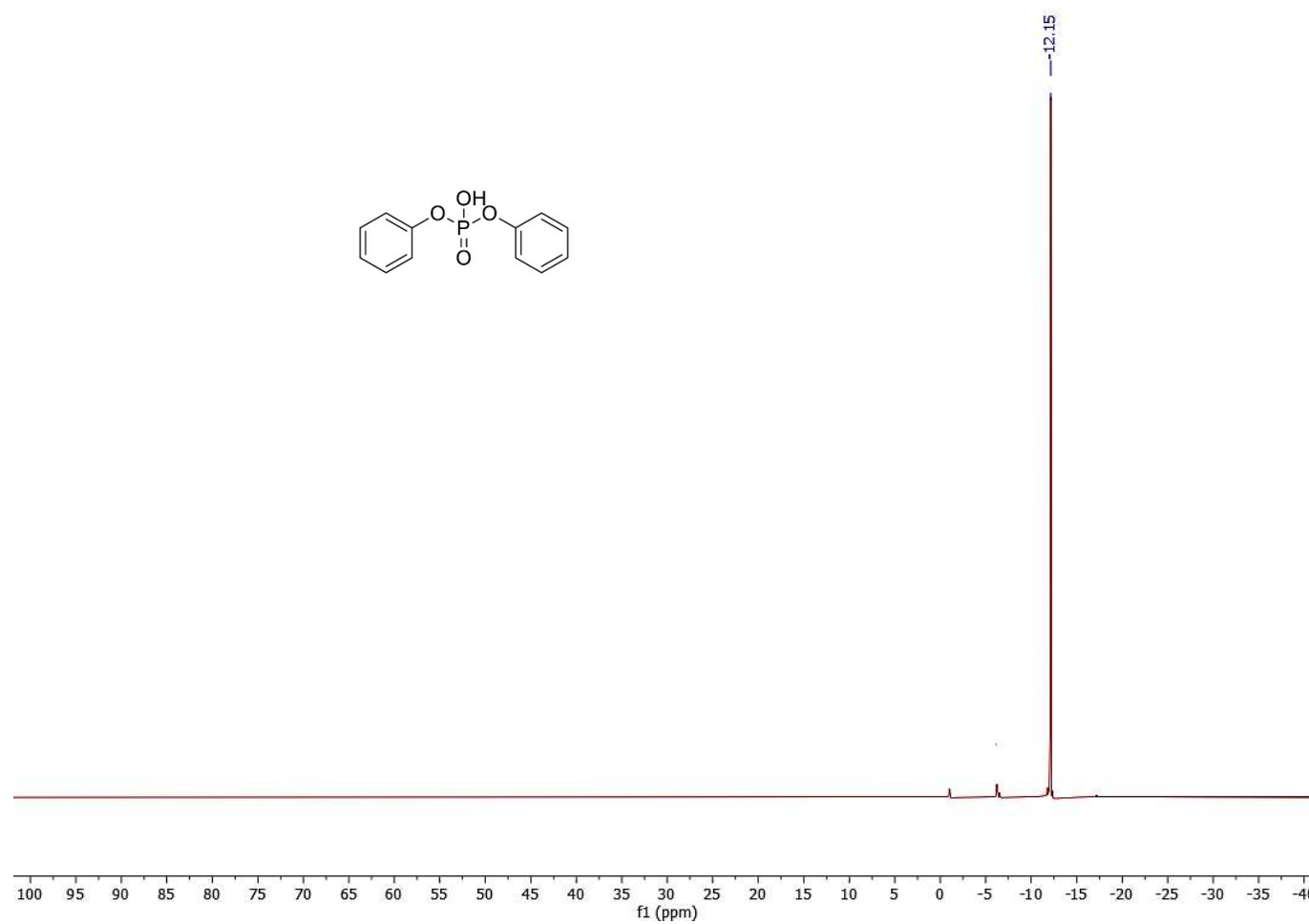


Figure S27: ³¹P NMR Spectra of 2j in DMSO-d₆

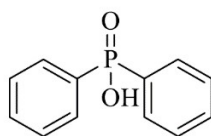


Figure S28: ^1H NMR Spectra of 2k in DMSO-d₆

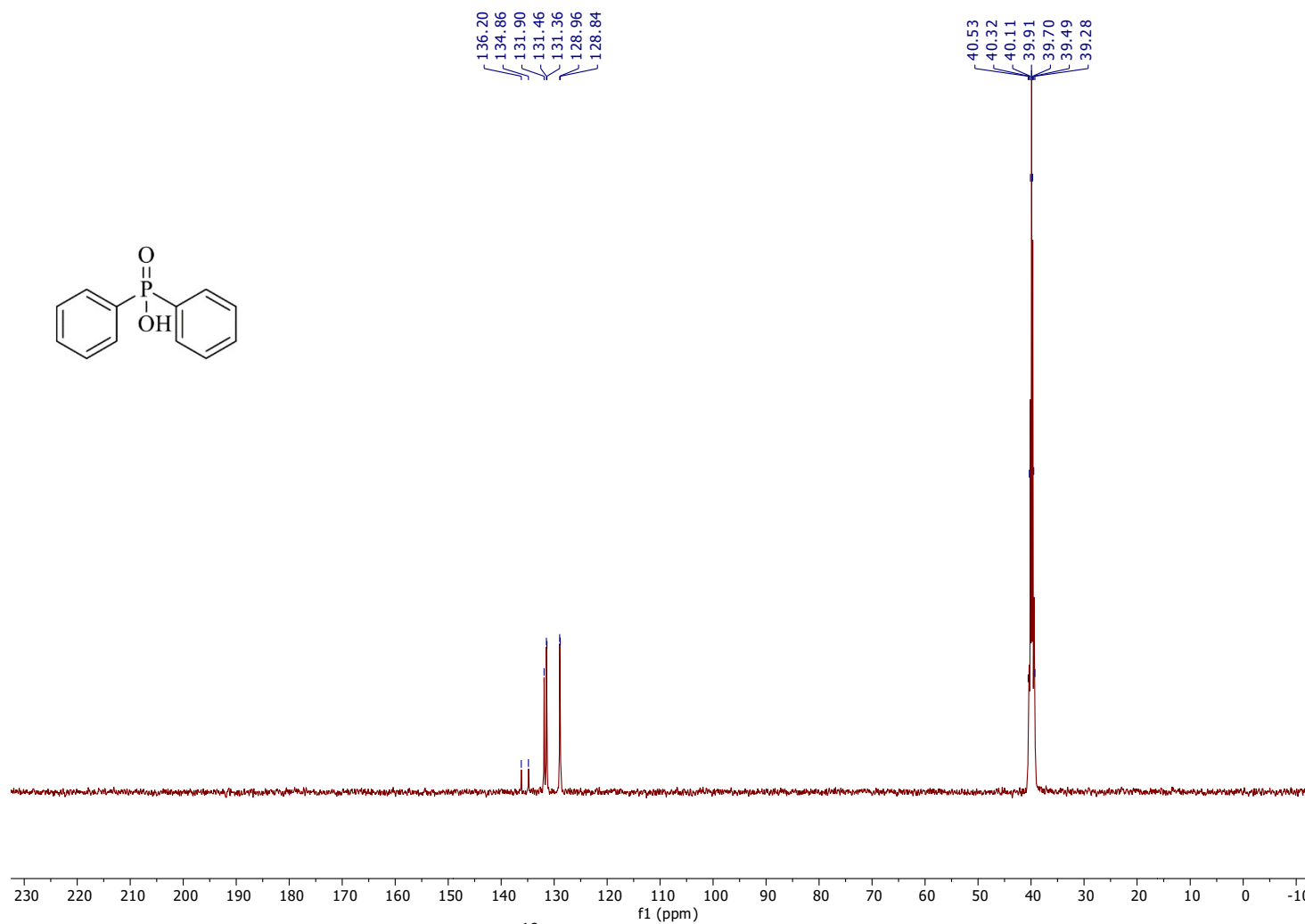


Figure S29: ¹³C NMR Spectra of 2k in DMSO-d₆

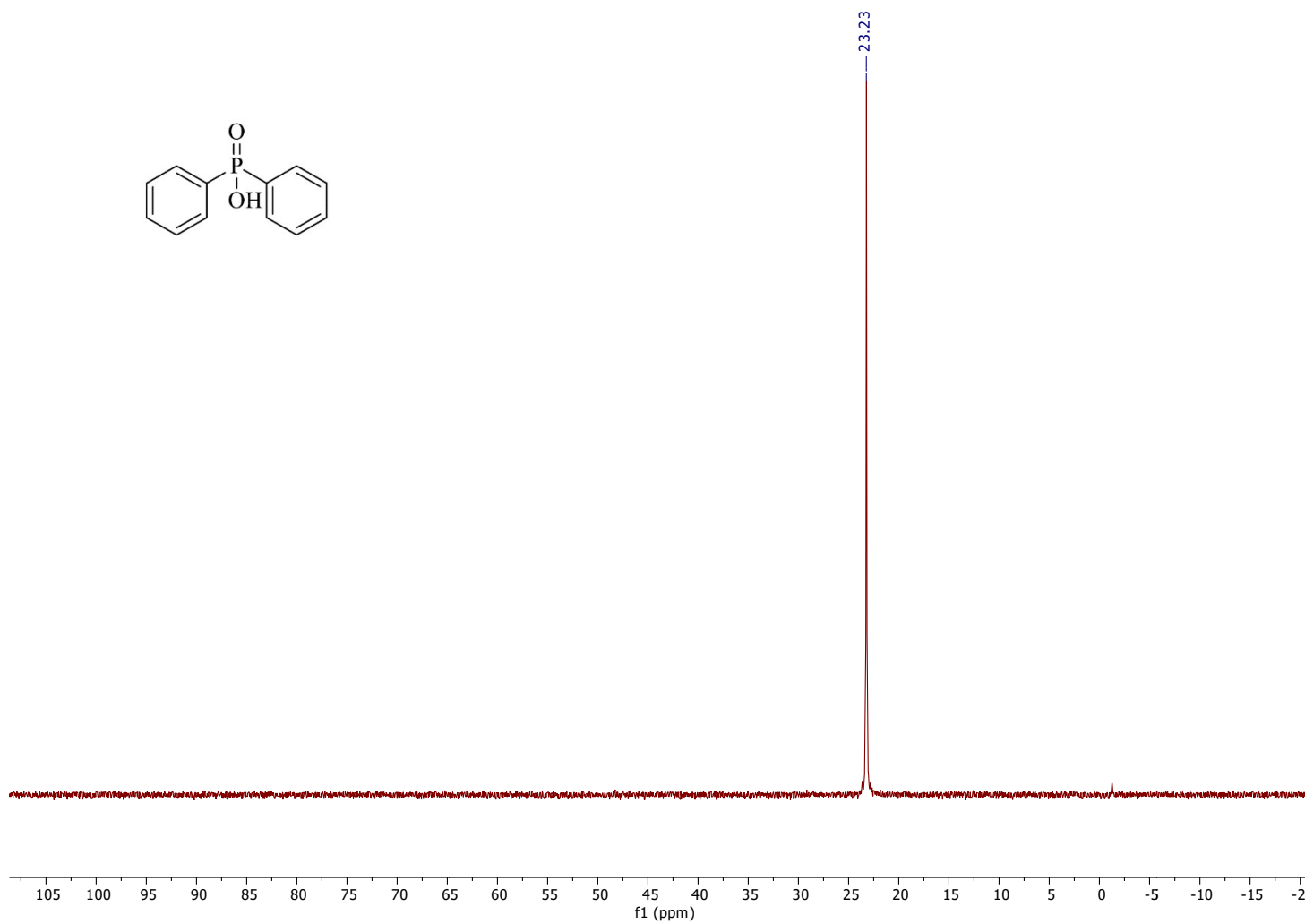


Figure S30: ^{31}P NMR Spectra of 2k in DMSO-d_6

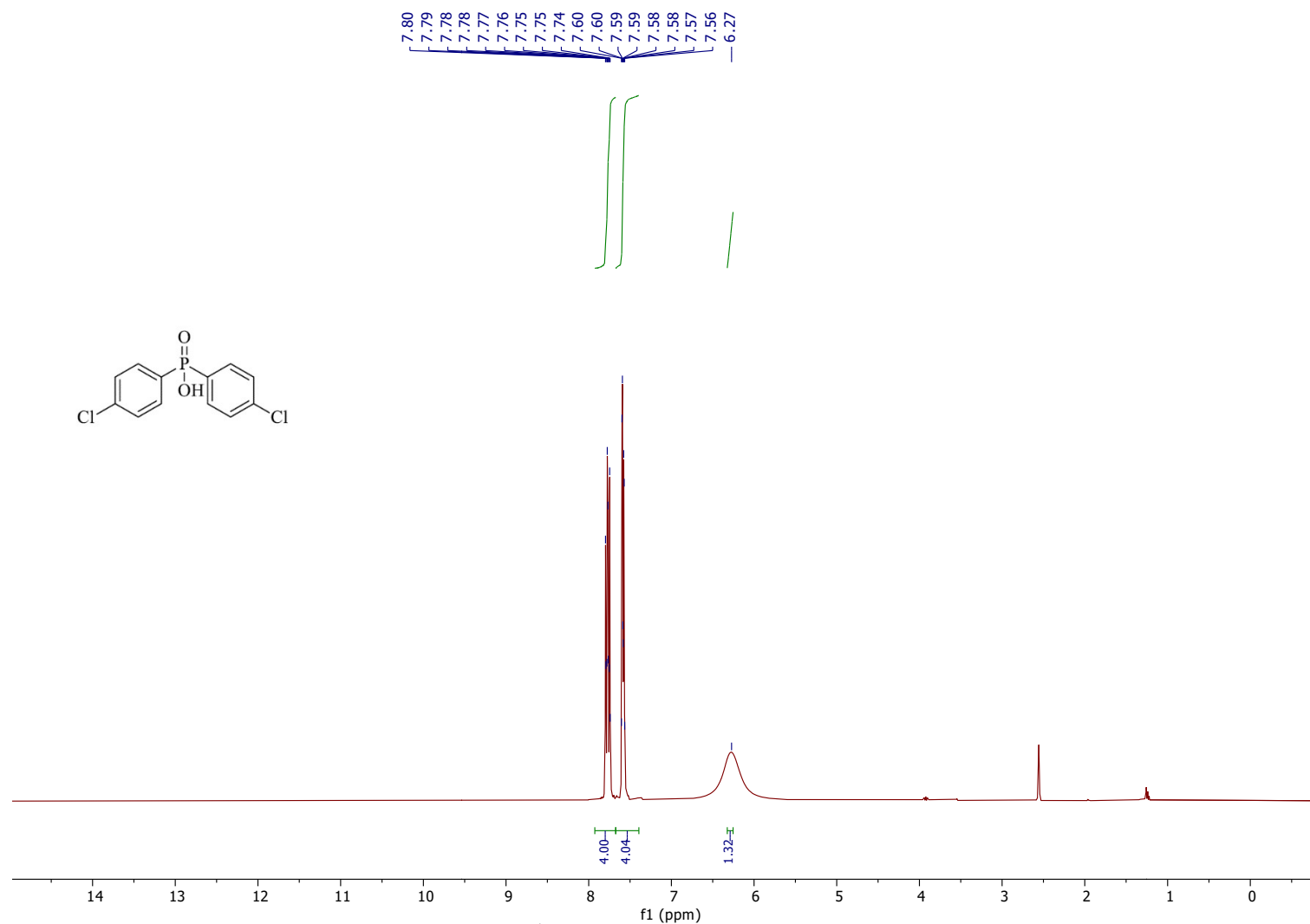


Figure S31: ¹H NMR Spectra of 2l in DMSO-d₆

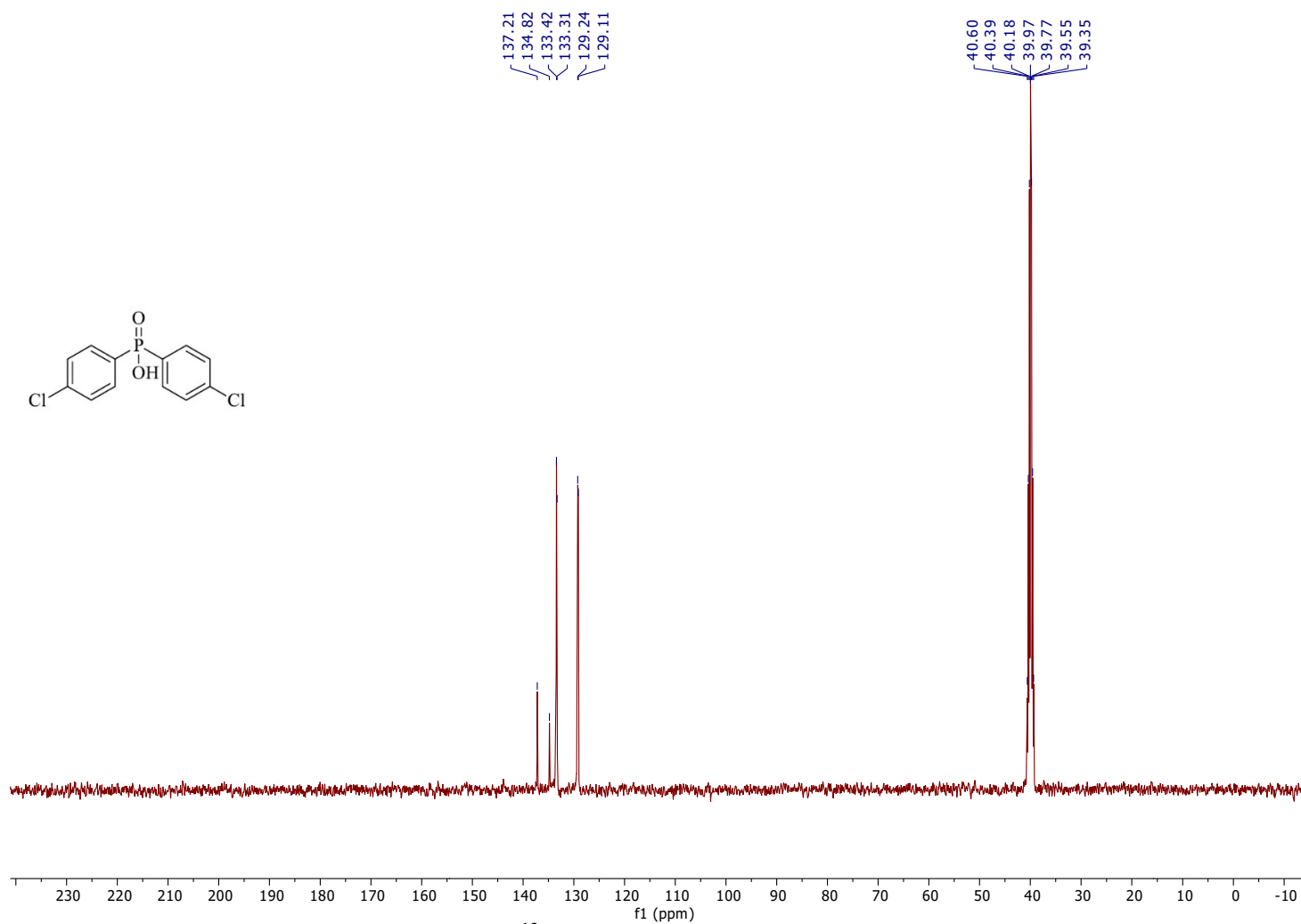


Figure S32: ¹³C NMR Spectra of 2l in DMSO-d6

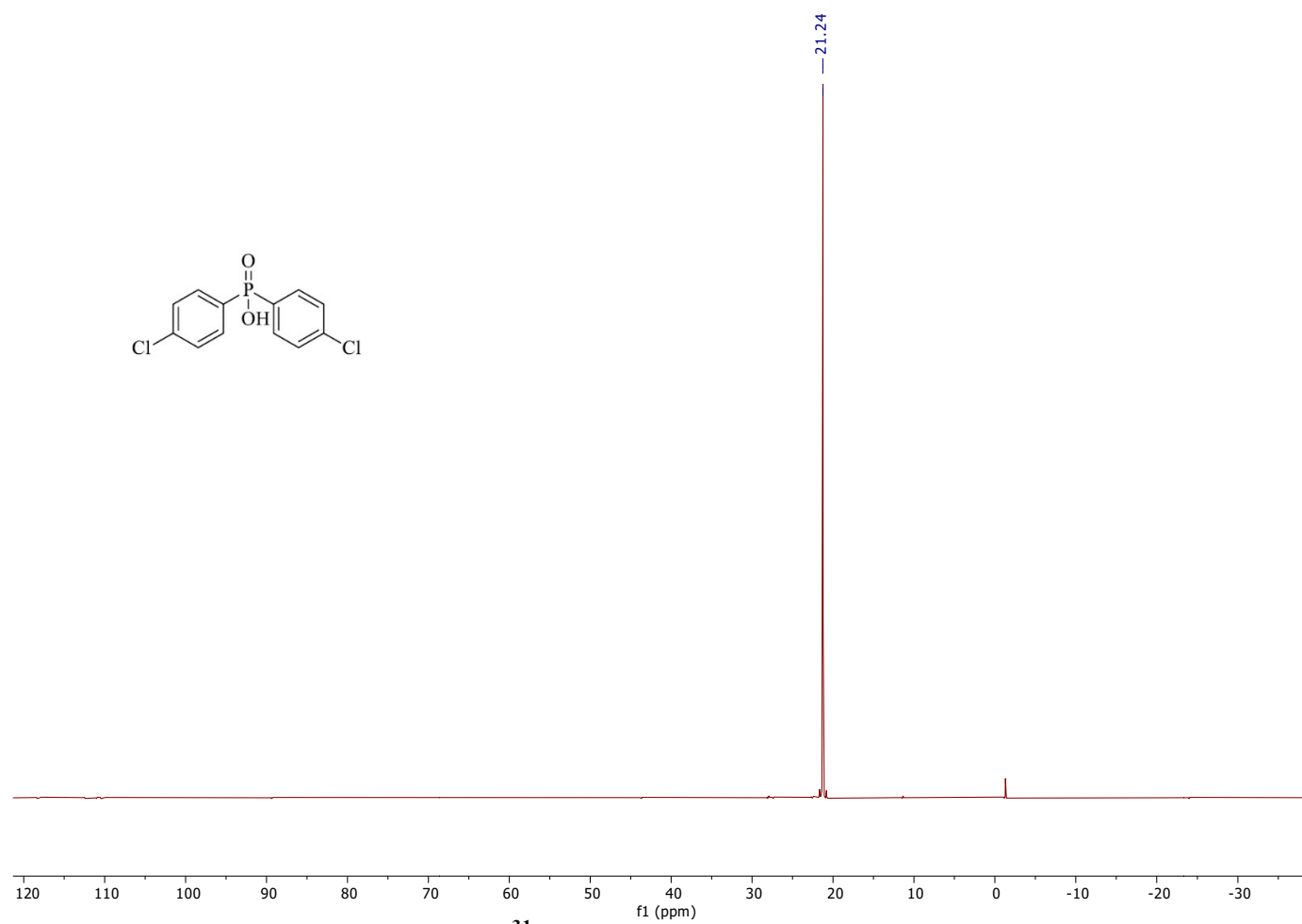


Figure S33: ^{31}P NMR Spectra of 2k in DMSO-d_6

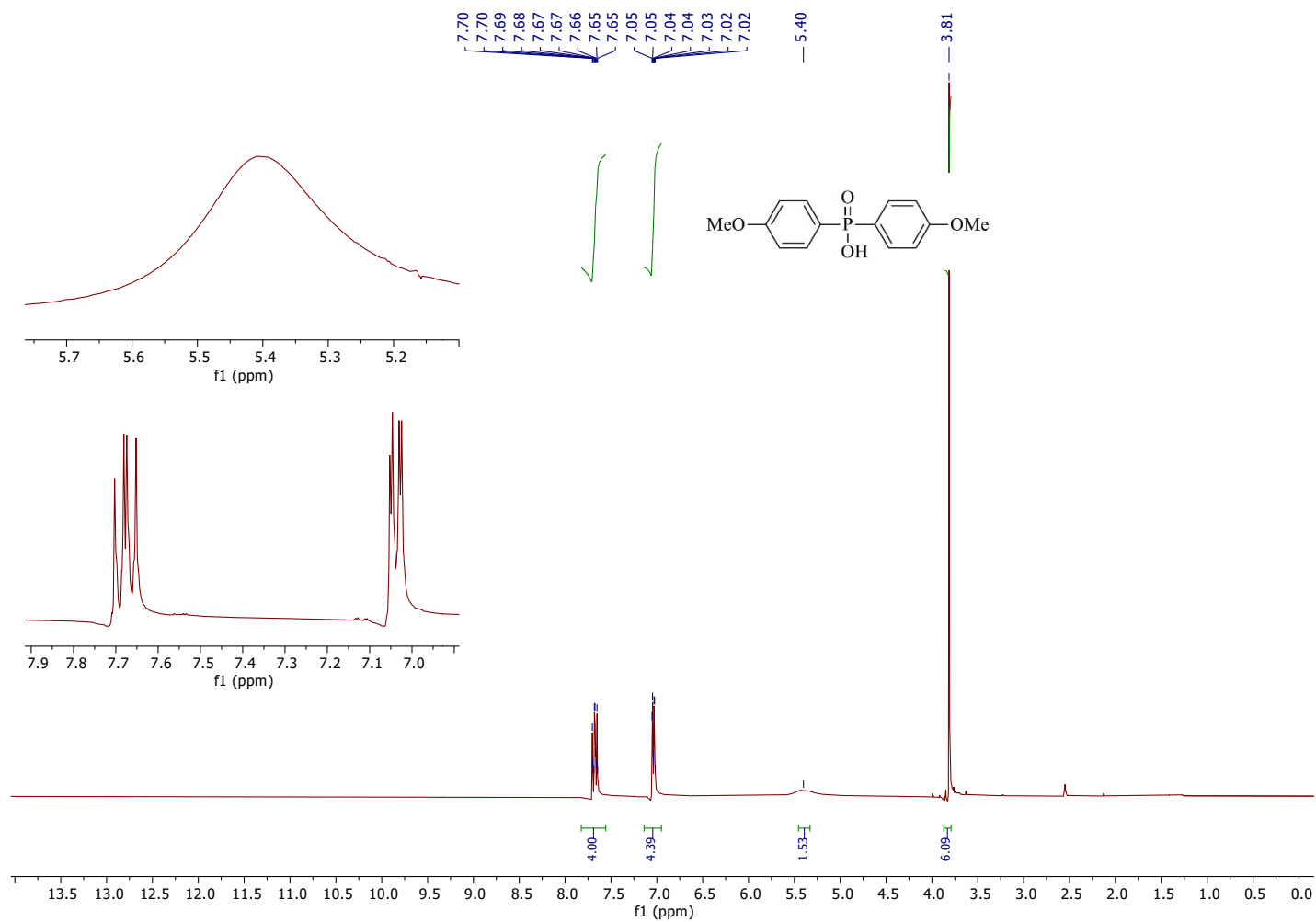


Figure S34: ¹H NMR Spectra of 2m in DMSO-d₆

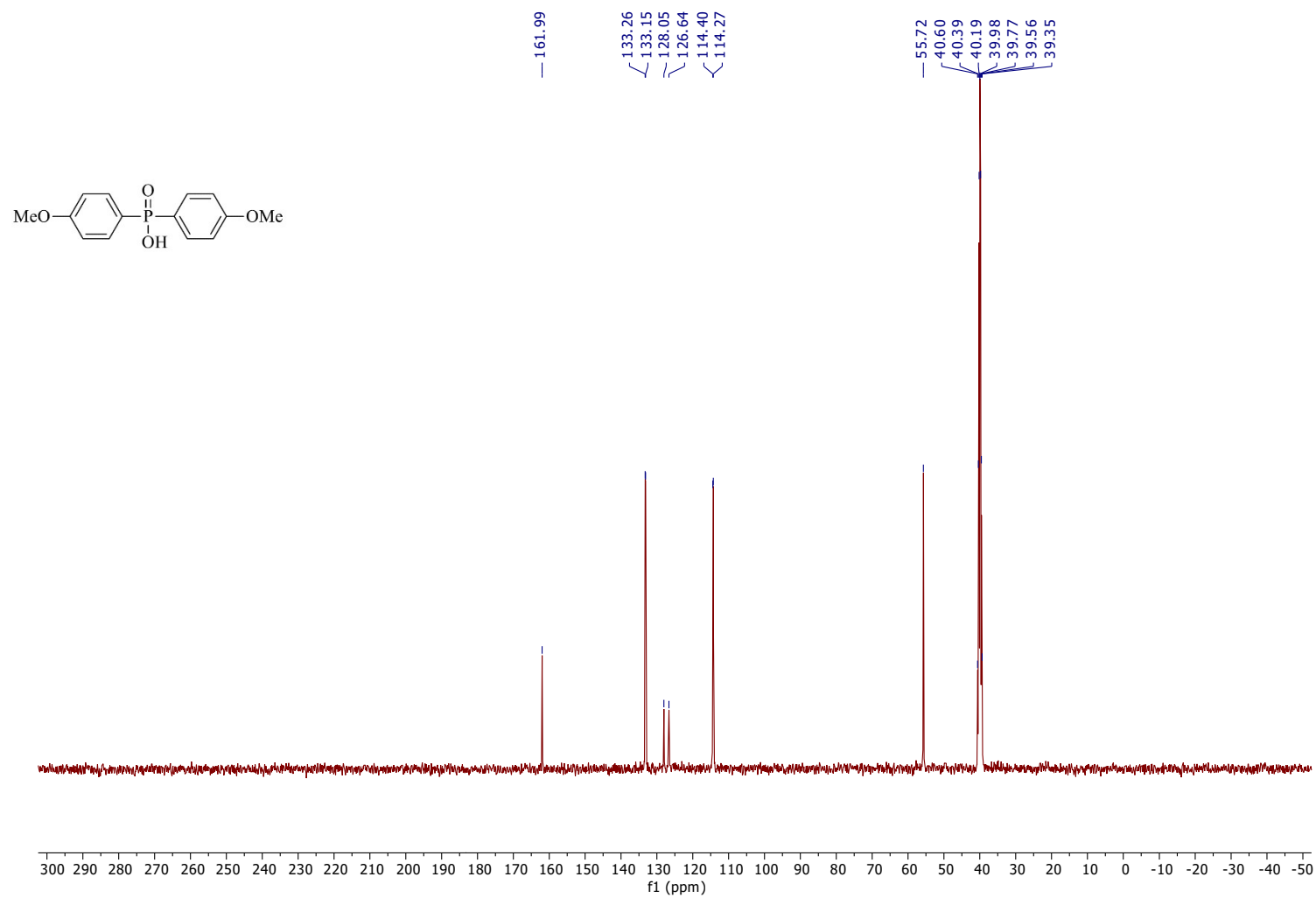


Figure S35: ^{13}C NMR Spectra of 2m in $\text{DMSO}-d_6$

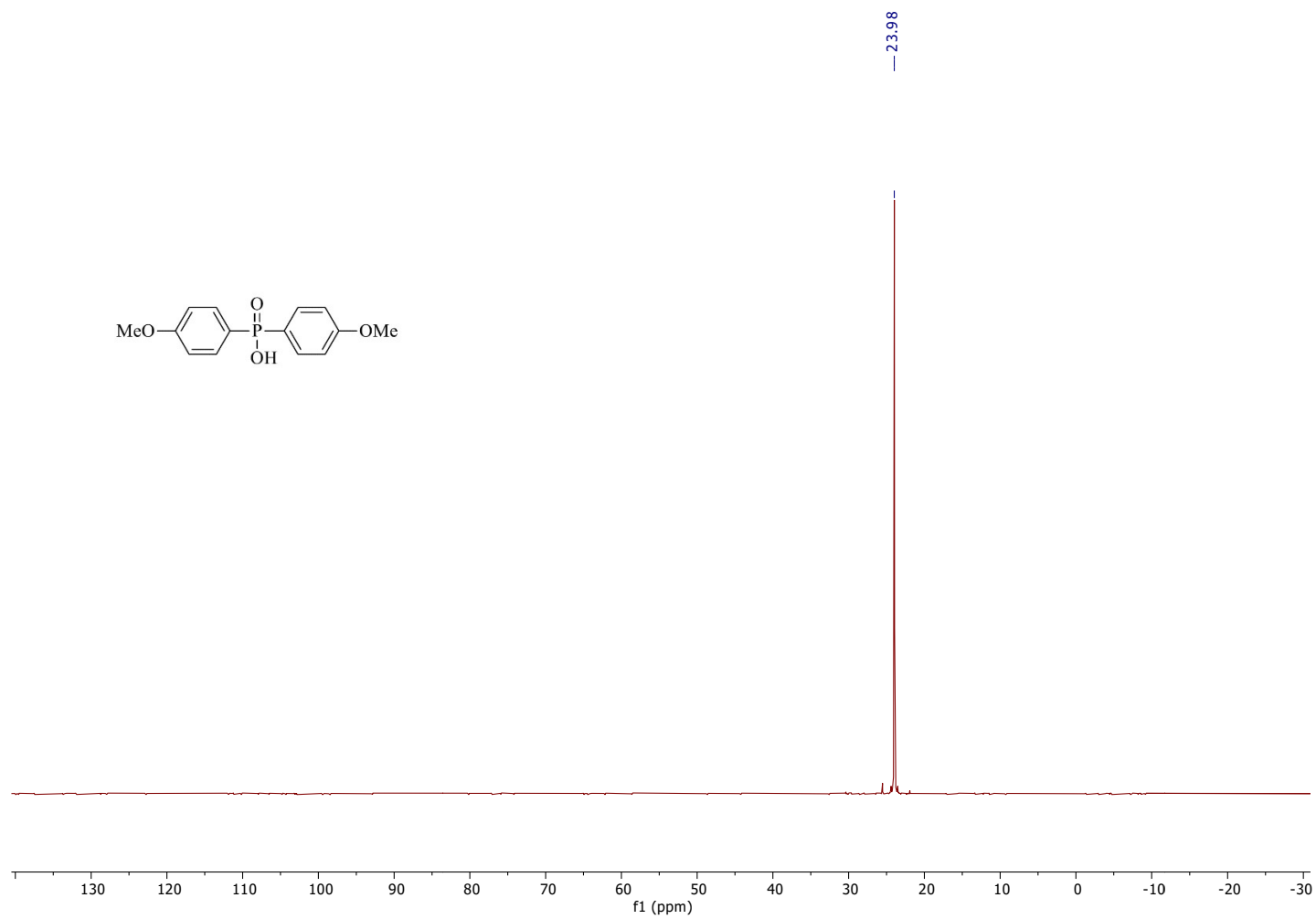


Figure S36: ^{31}P NMR Spectra of 2m in DMSO- d_6

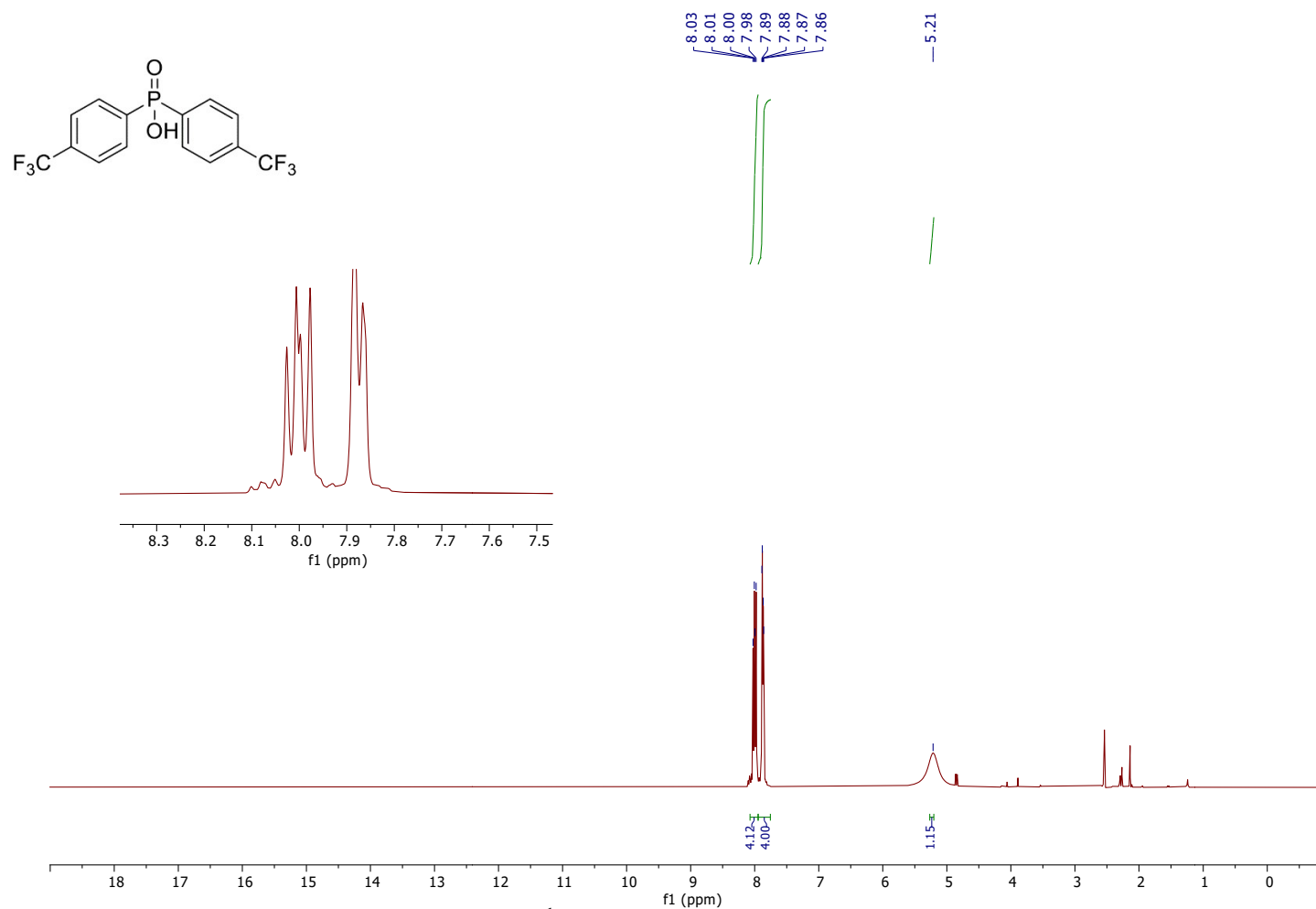


Figure S37: ¹H NMR Spectra of 2n in DMSO-d₆

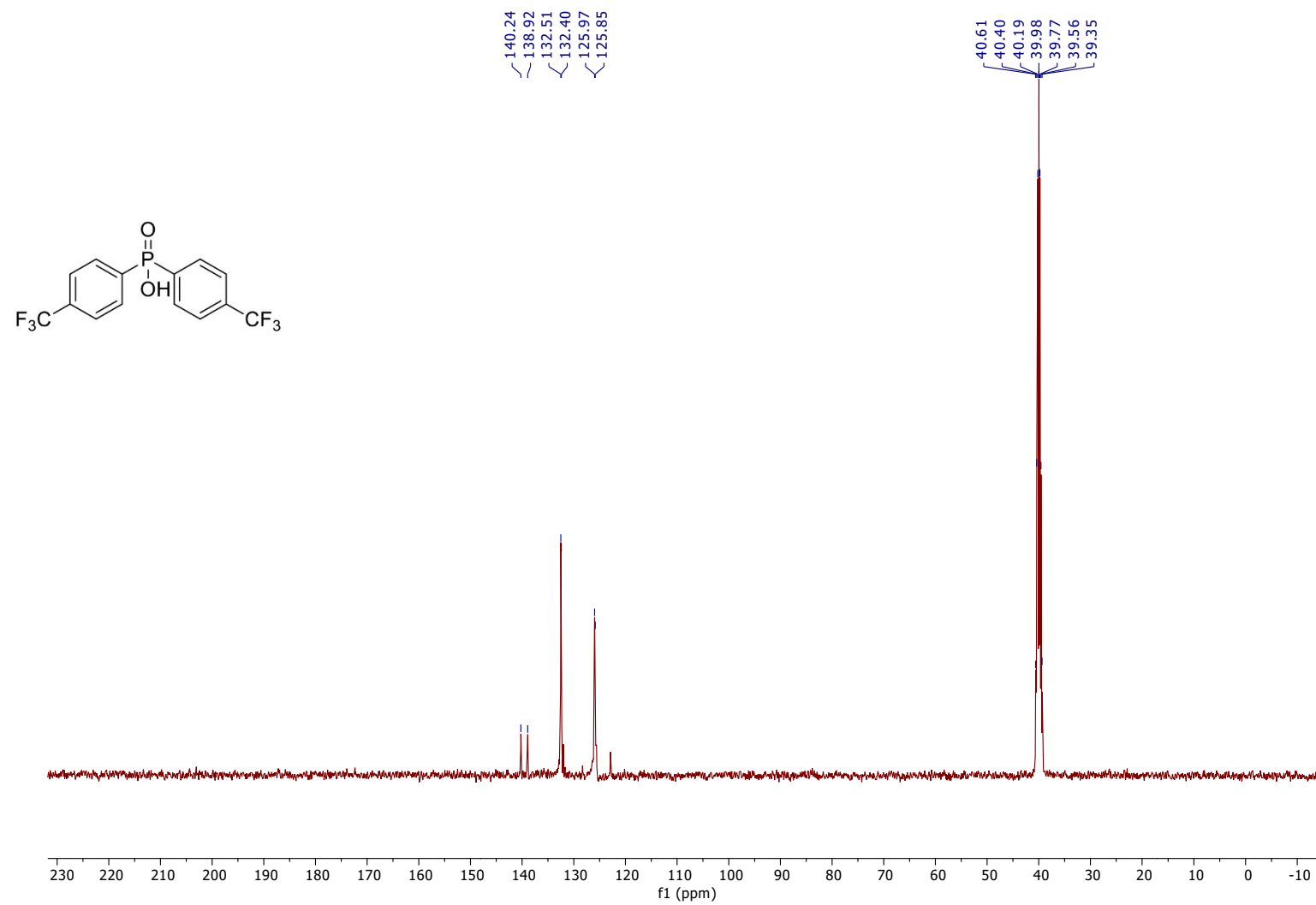


Figure S38: ^{13}C NMR Spectra of 2n in DMSO-d₆

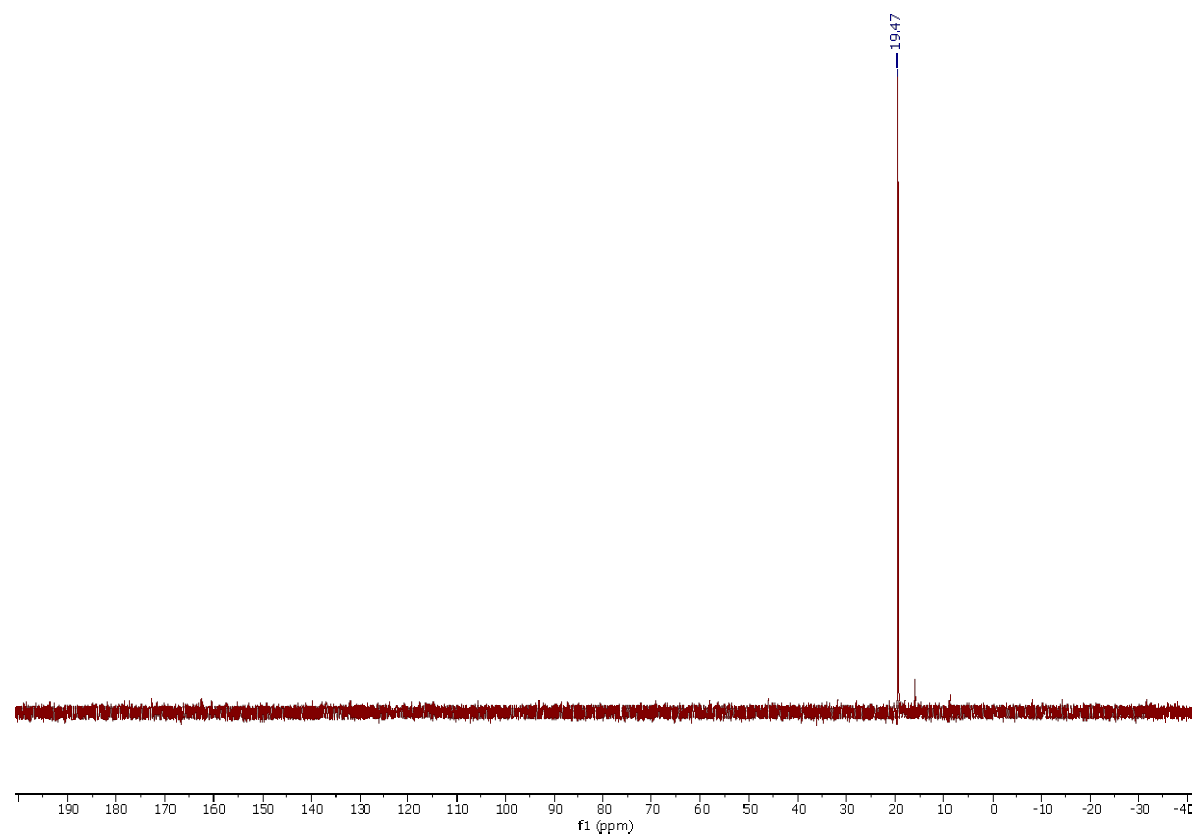


Figure S39: ^{31}P NMR Spectra of **2n** in DMSO- d_6

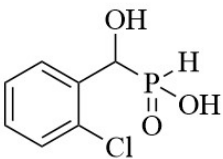


Figure S40: ^1H NMR Spectra of 3 in DMSO- d_6

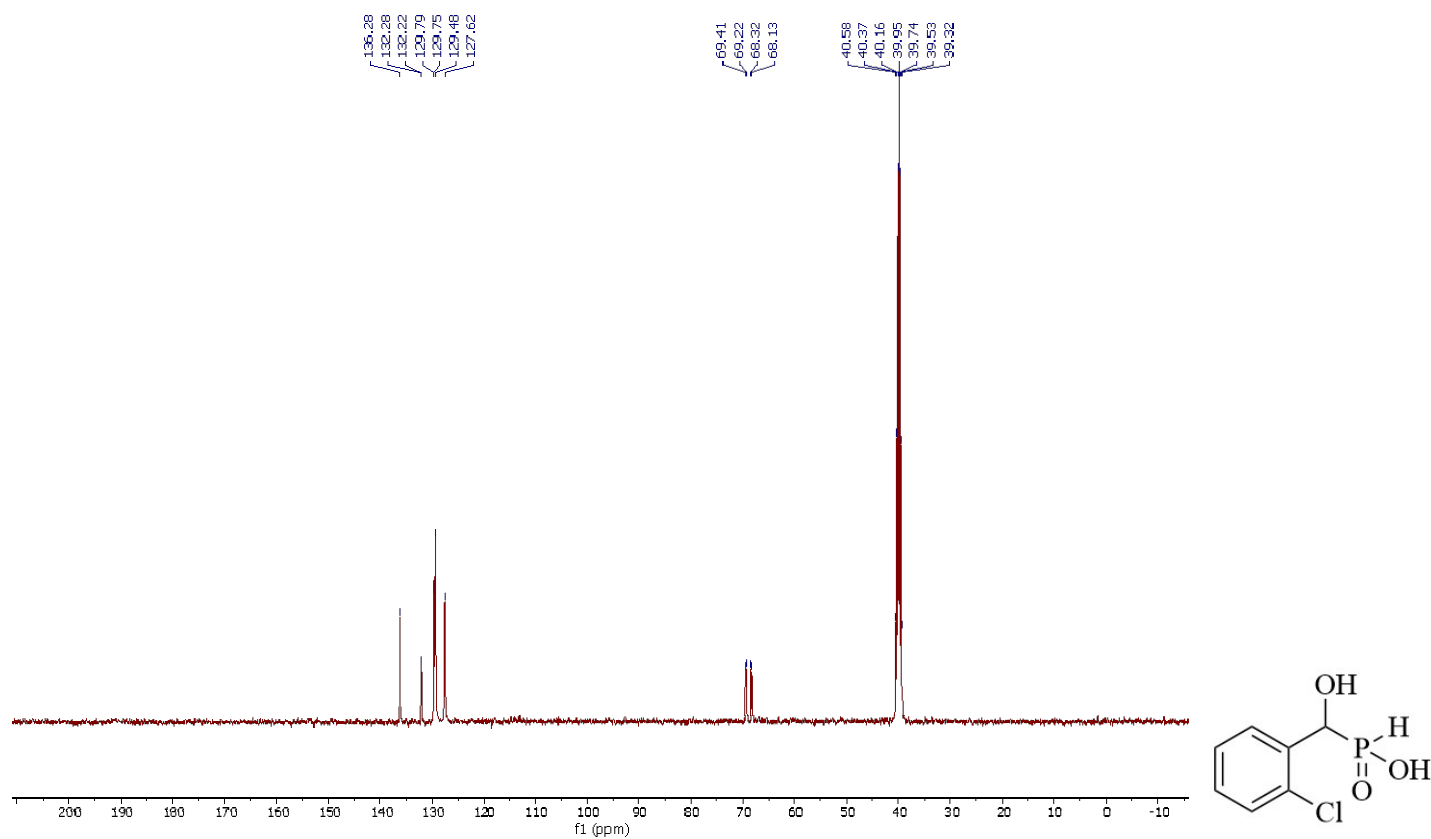


Figure S41: ¹³C NMR Spectra of 3 in DMSO-d₆

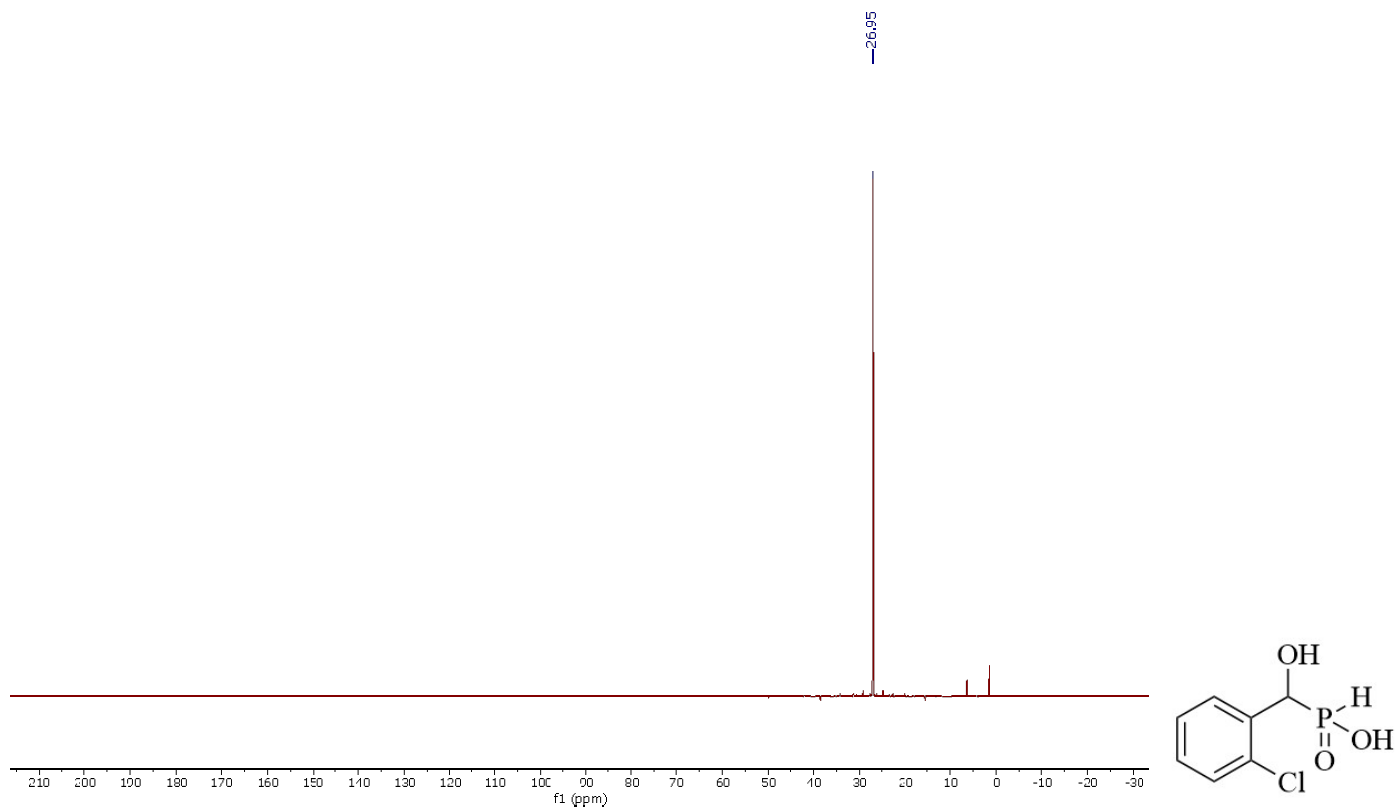


Figure S42: ^{31}P NMR Spectra of 3 in DMSO- d_6

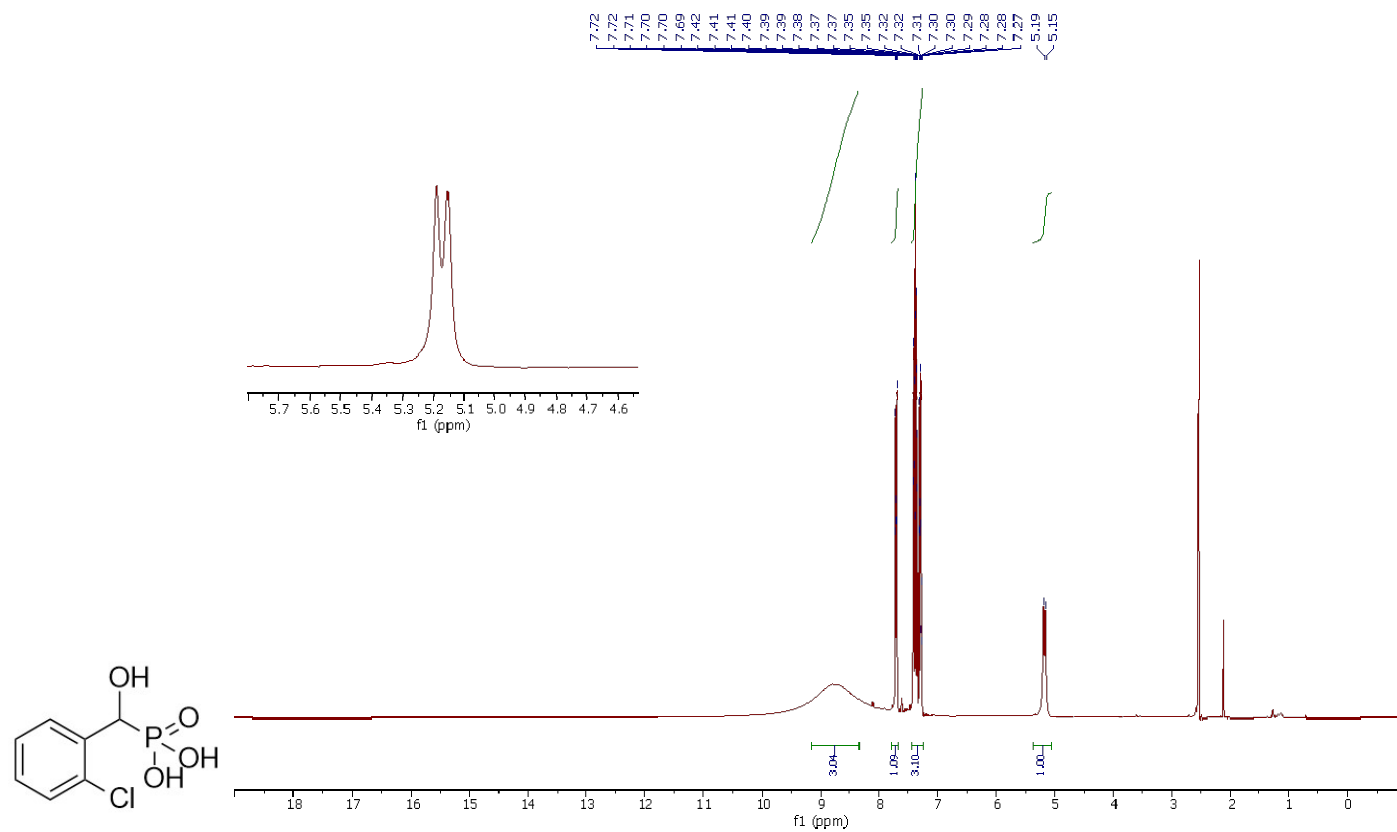


Figure S43: ¹H NMR Spectra of 4 in DMSO-d₆

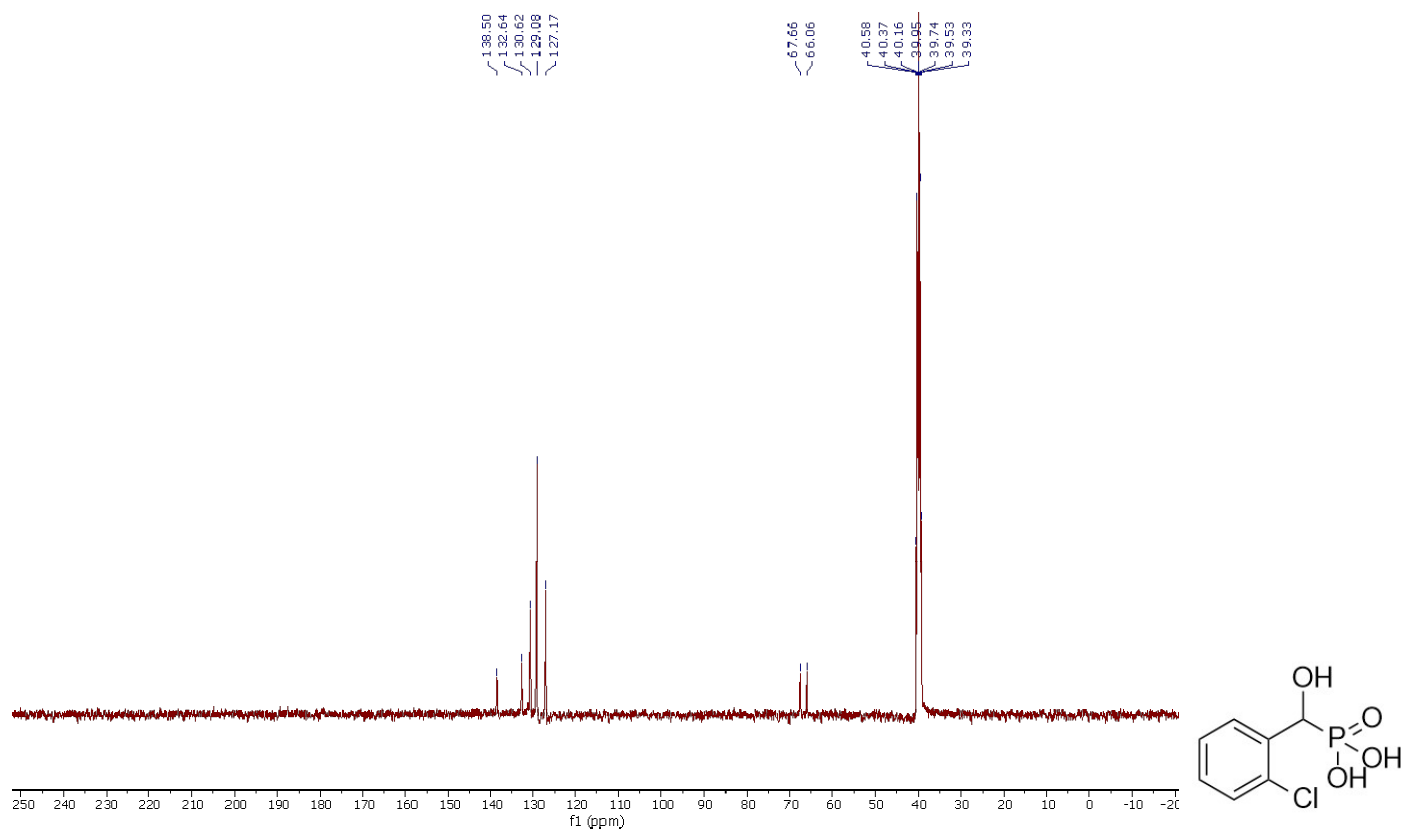


Figure S44: ¹³C NMR Spectra of 4 in DMSO-d₆

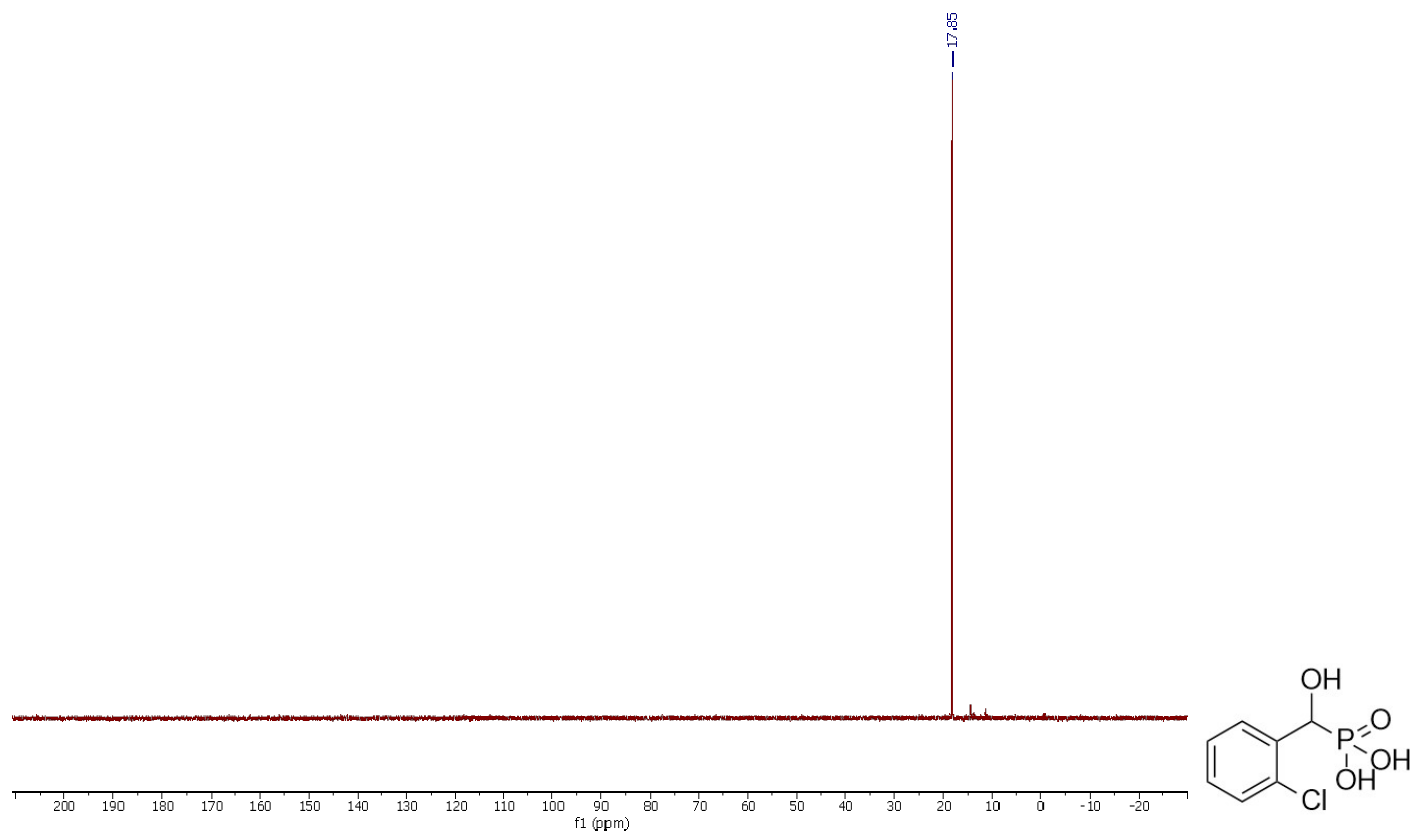


Figure S45: ^{31}P NMR Spectra of 4 in DMSO-d6

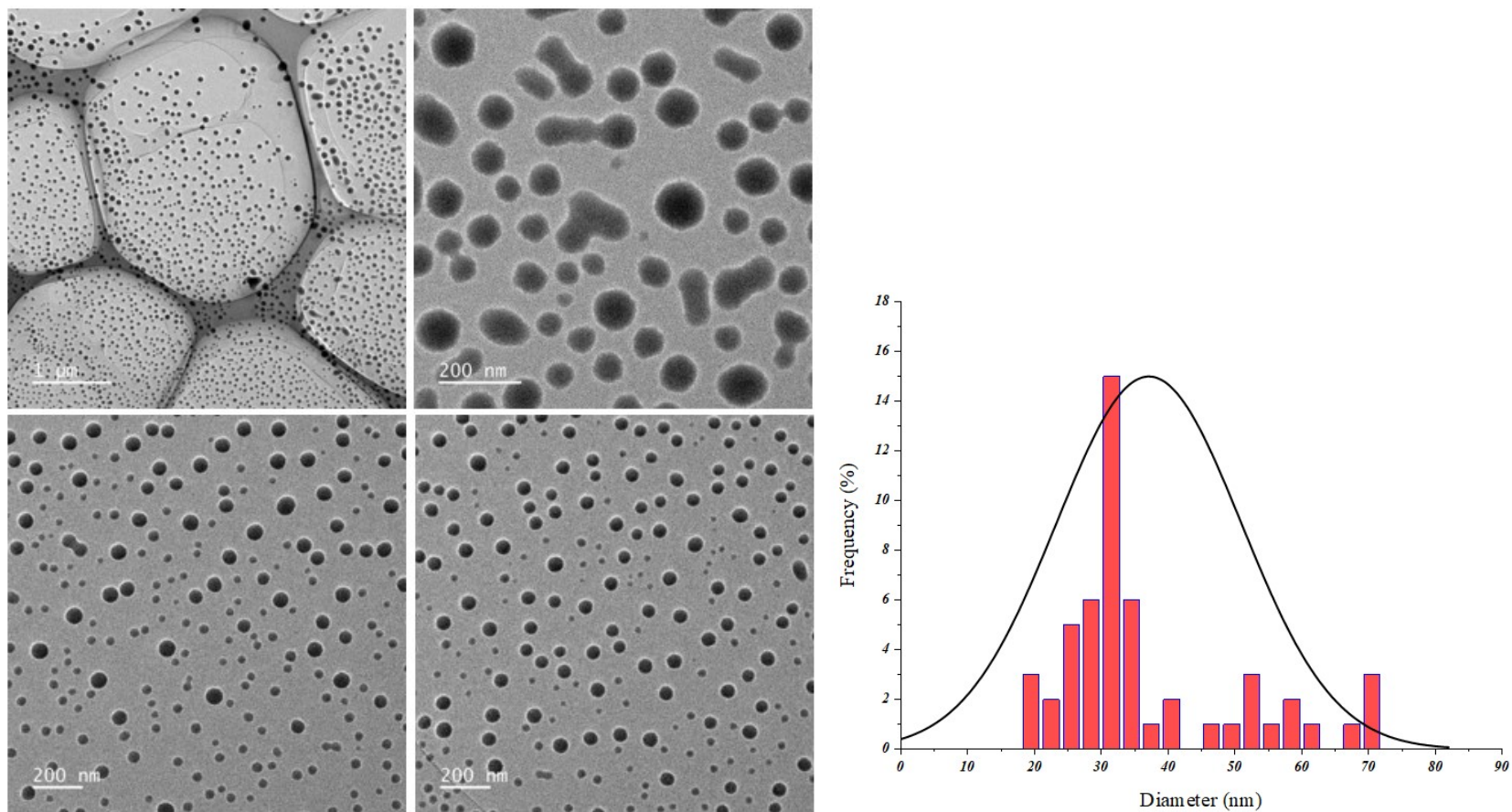


Figure S46. TEM images of DMP-Se-NPs and Distribution Diagram of DMP-Se-NPs

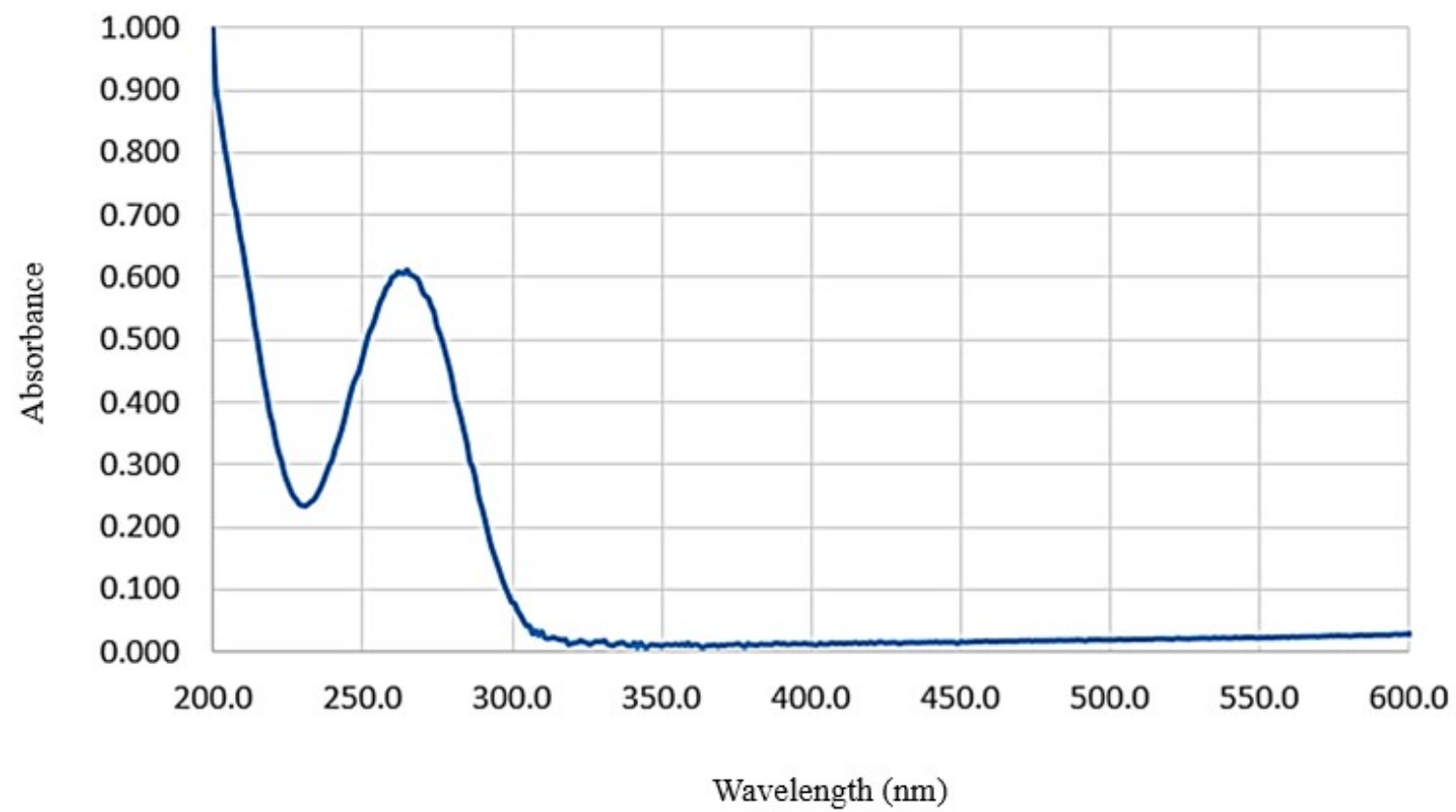


Figure S47: Ultraviolet-visible of DMP-Se-NPs

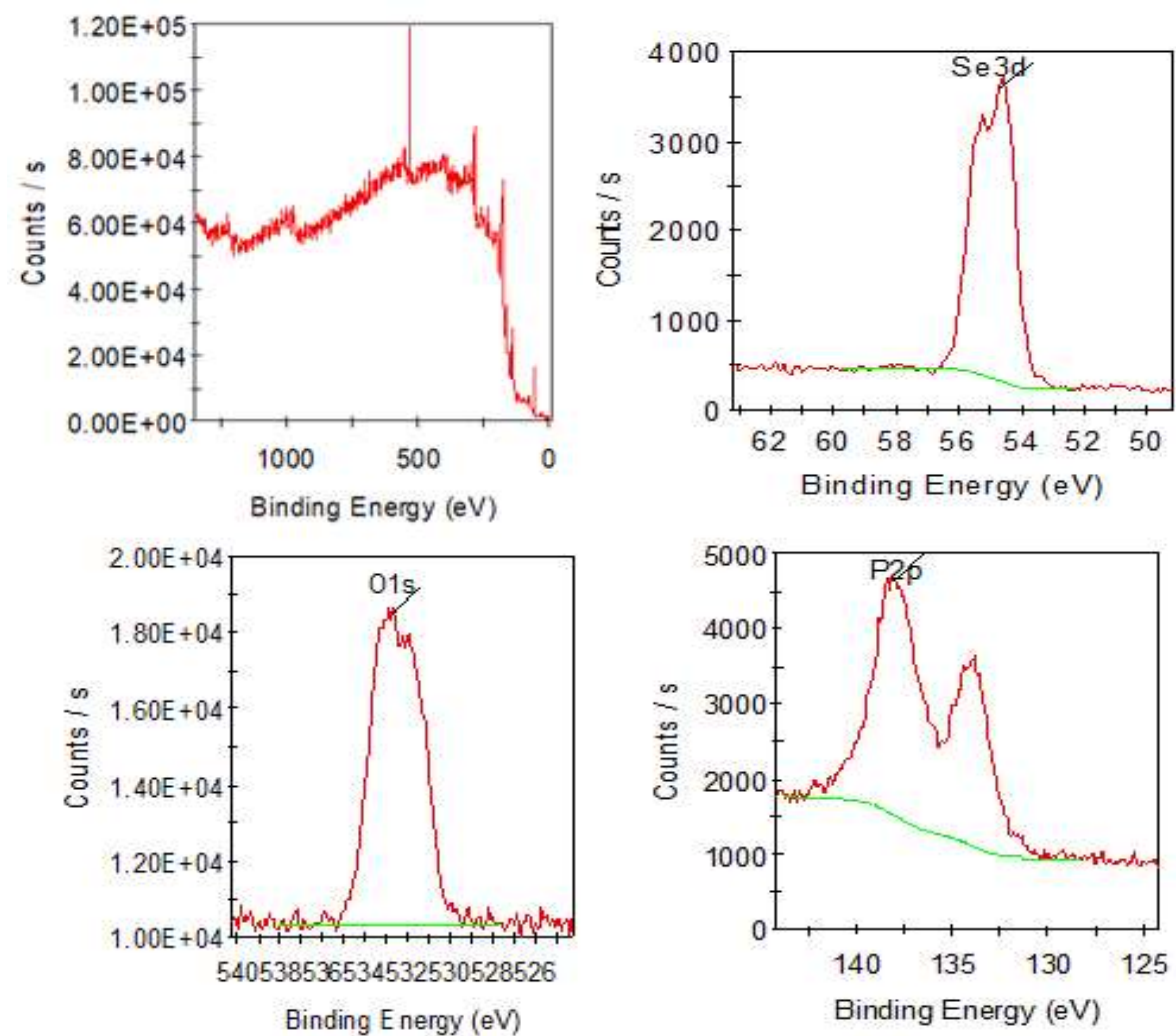


Figure S48: XPS analysis of DMP-Se-NPs

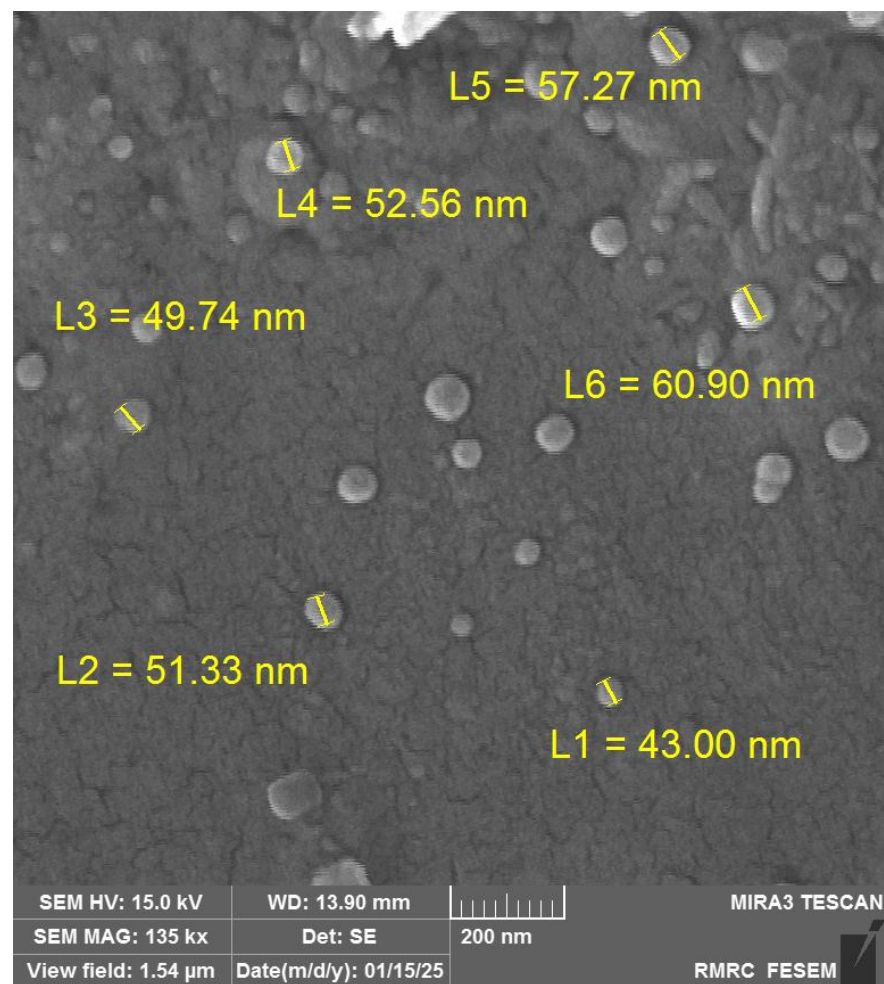


Figure S49: FE-SEM image of β -CD@Se NPs

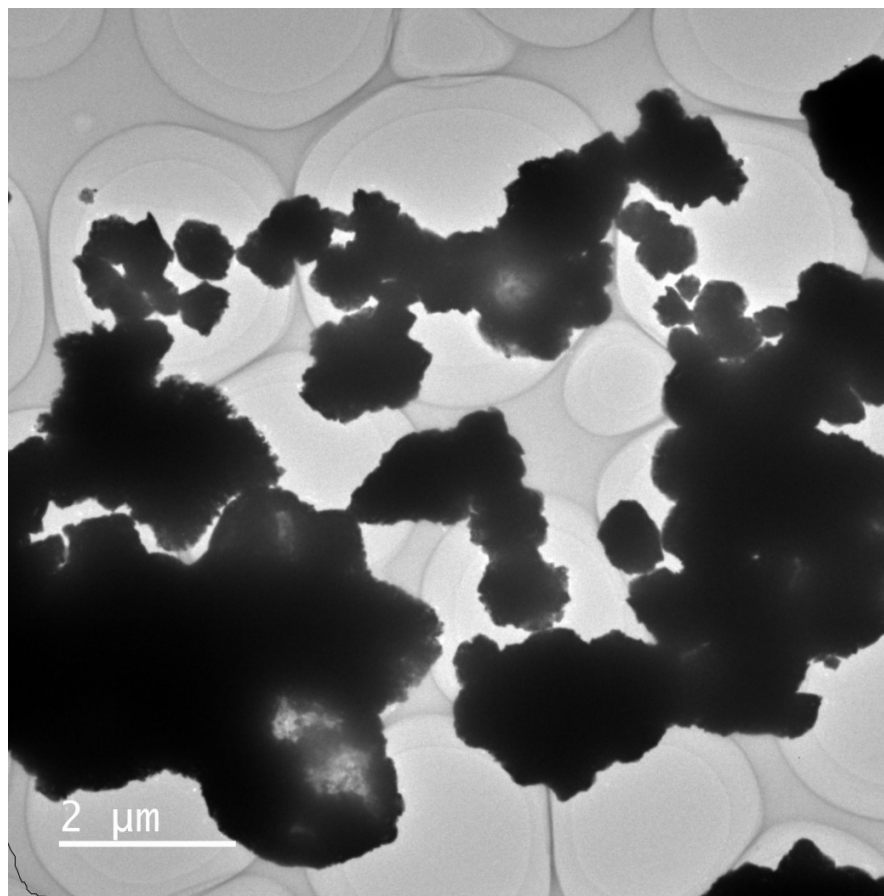


Figure S50: TEM of a sample of aggregated Se-NPs

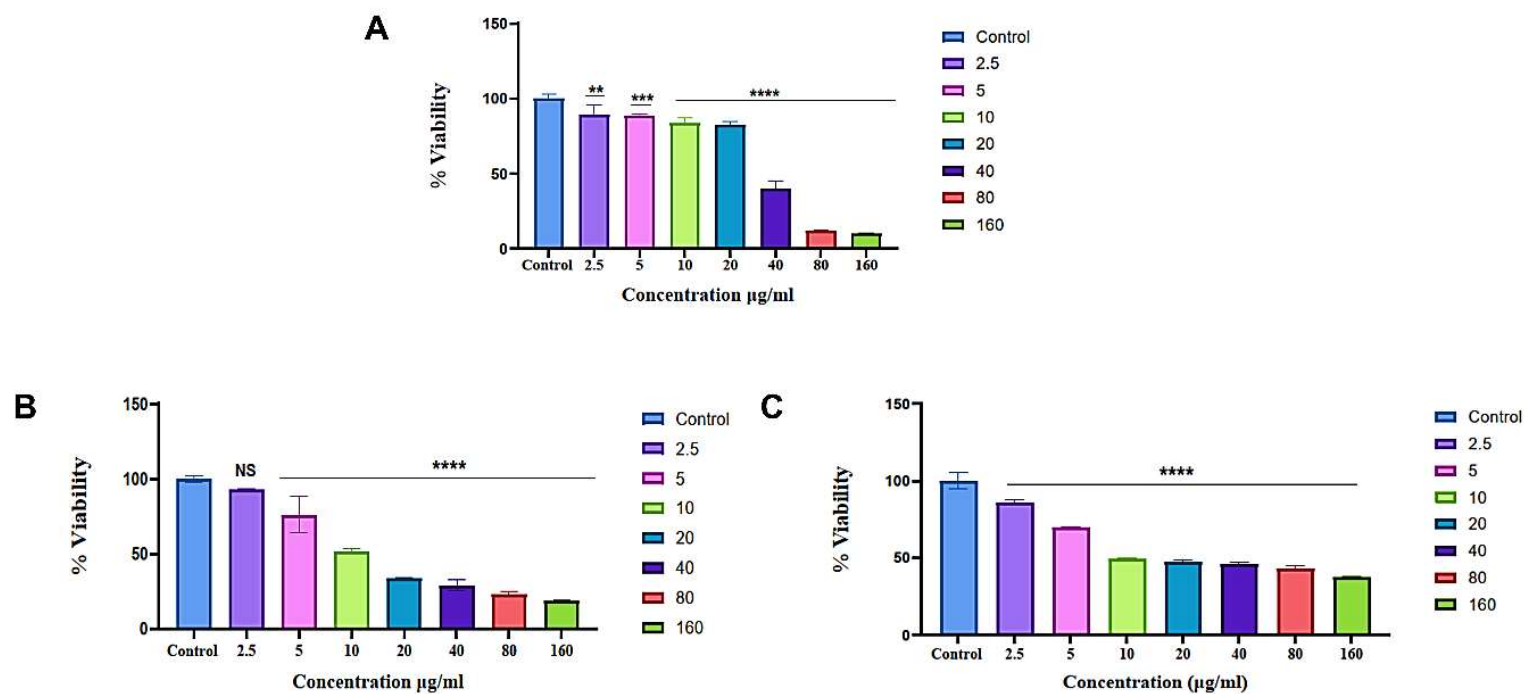


Figure S51: Cell viability after treatment with different concentrations of Se NPs (2.5, 5, 10, 20, 40, 80 and 160 µg/ml) after 24h for **A.** 4T1 **B.** MCF-7 and **C.** MDA-MB-231 cells. Data is represented as mean \pm SD. SD: standard deviation.(magnification \times 100)

** $P_{\text{value}} < 0.01$ *** $P_{\text{value}} < 0.001$ **** $P_{\text{value}} < 0.0001$

Anti-cancer properties: Experimental part

Cell culture

Mouse breast cancer cell line, 4T1 and human breast cancer cell lines, MCF7 and MDA-MB-231 were cultured in DMEM supplemented with 10%(v/v) fetal bovine serum (FBS) and 1%(v/v) penicillin/streptomycin. Cells were maintained in an incubator with temperature of 37°C and a humidified environment of 5% CO₂. The culture media was refreshed every two days.

Cell survival assay

The viability of 4T1, MCF7 and MDA-MB-231 cells in different concentrations of Se nanoparticles (2.5, 5, 10, 20, 40, 80 and 160 µg/ml) in comparison with the control group (non-treated) was determined via 3-(4,5-dimethylthiazol-2-yl)-2,5-diphenyltetrazolium bromide (MTT) assay. Briefly, after reaching a confluency of 80%, cells were trypsinized and 10⁴ cells were seeded in a 96-well cell culture plate, then 100 microliters of culture medium containing 10% FBS was added to them. After 24 hours, the supernatant was removed and cells were treated with Se NPs dissolved in DMEM culture medium at defined concentrations for 24 h. The MTT assay was performed by removing culture media and adding 100 µl MTT solution in DMEM (final concentration of 0.5 mg/mL MTT) to each sample. After 4 h incubation in a dark place, the supernatant was removed and 0.05 ml DMSO was added to each well. In the final step, the absorbance of samples was read at 570 nm using a Microplate Reader (ELX800; BioTeK, Winooski, VT). The assay was performed in triplicate.

The viability of mouse and human breast cancer cell lines in different concentrations of Se NPs was evaluated using the MTT assay after 24 hours. The results depicted in Figure S51 demonstrate that Se NPs suppressed the proliferation of breast cancer cells in a concentration-dependent manner. The toxic effect of cyclodextrin-encapsulated Se NPs on 4T1 cells was initiated in concentration of 2.5 µg/mL of the cyclodextrin-encapsulated Se NPs ($P_{\text{value}}=0.0016$). A concentration of 5 µg/mL of these NPs had a lethal effect on 4T1 cells with a P value of 0.0006, and from a concentration of 10, this lethal effect increased significantly ($P_{\text{value}} < 0.0001$). Also, in

the MCF-7 cell line, the concentration range of 10-160 $\mu\text{g/mL}$ of these particles significantly reduced cell viability compared to the control group (P value <0.0001). Similar results were also observed in the concentration range of 2.5-160 $\mu\text{g/mL}$ on the MDA-MB-231 cell line (P value <0.0001).

Electrochemical experimental part

The electrochemical properties were studied using Autolab PGSTAT 101 with NOVA software in a typical three-electrode voltammetric cell consisting of a glassy carbon disk (GC, 1.8 mm diameter), Ag/AgCl and Pt wire as working, reference and counter electrode, respectively. Before recording each voltammogram, the GC electrode was polished with 0.05 μm alumina powder. The electrode was then thoroughly washed with distilled water.

Electrochemical studies

The oxidative and reductive properties of SeO_2 were initially studied using cyclic voltammetry. Fig. S49 presents cyclic voltammograms of 50 mM SeO_2 in water containing 0.1 M KCl as supporting electrolyte in two different ranges of potential. By scanning the potential toward negative direction from 0 to -0.9 V vs. Ag/AgCl (curve a in Fig. S49), the voltammogram shows one sharp peak (C_1) at -0.67 V which corresponds to the electrochemical reduction of SeO_2 to Se^0 . During the reverse scan one anodic signal with a sharp adsorption feature appeared at 1.26 V, which is associated with the oxidation of the electrogenerated Se^0 . The curve b in Fig. S49 exhibits a cyclic voltammogram of SeO_2 at the same situation of curve a by recording toward the positive direction, from 0 to +1.5 V. Given that the center of Se in SeO_2 is in the highest oxidation state, no anodic signal was observed in curve b. The

data demonstrate that the A_1 peak arises from the oxidation of the cathodically generated Se^0 . Curve c in Fig. S49 is related to the voltammogram of 100 mM diethylphosphite. The inconsiderable current in the voltammogram shows that diethylphosphite is electro-inactive in the studied range of 0 to +1.5 V.

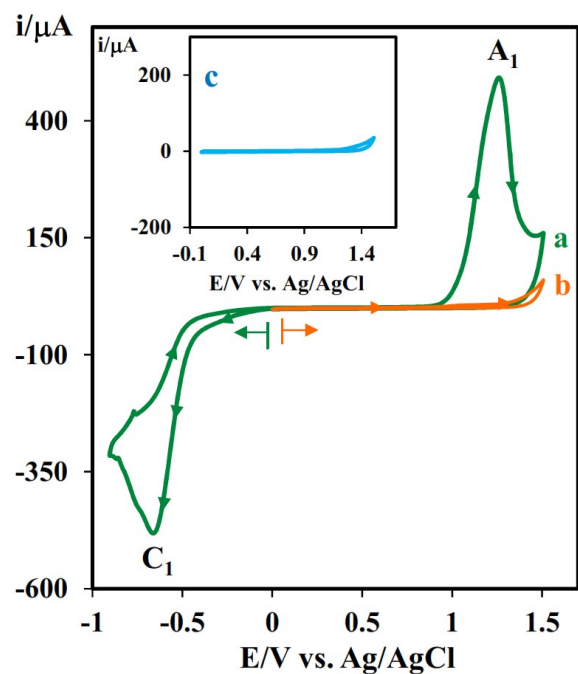


Figure S52. Cyclic voltammograms of (a and b) 50 mM SeO_2 at different ranges of potential and (c) 100 mM diethylphosphite at glassy carbon electrode in water containing 0.1 M KCl at scan rate of 100 mV/s. The cross indicates the starting potential. The arrows show the direction of the potential scan.

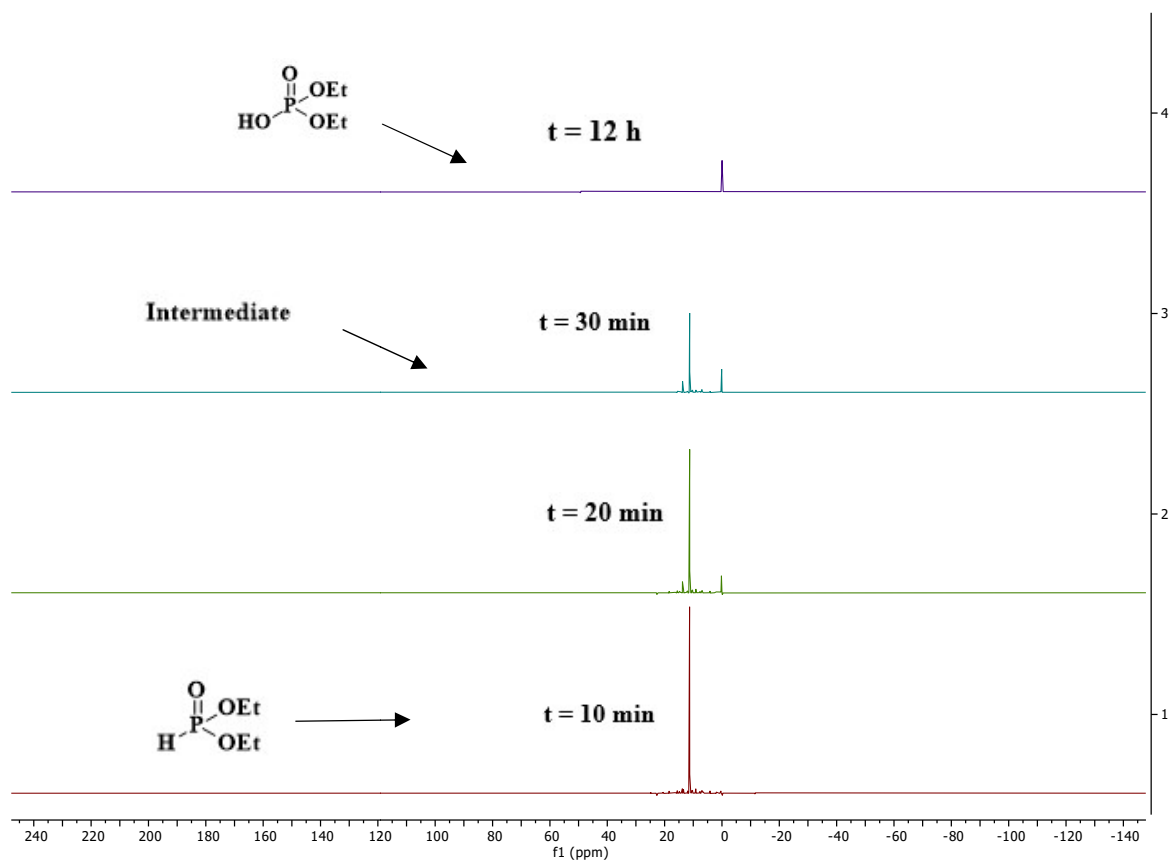


Figure S53: ^{31}P NMR Spectra of the conversion of the compound 1a to 2a in the presence of SeO_2 in D_2O at rt

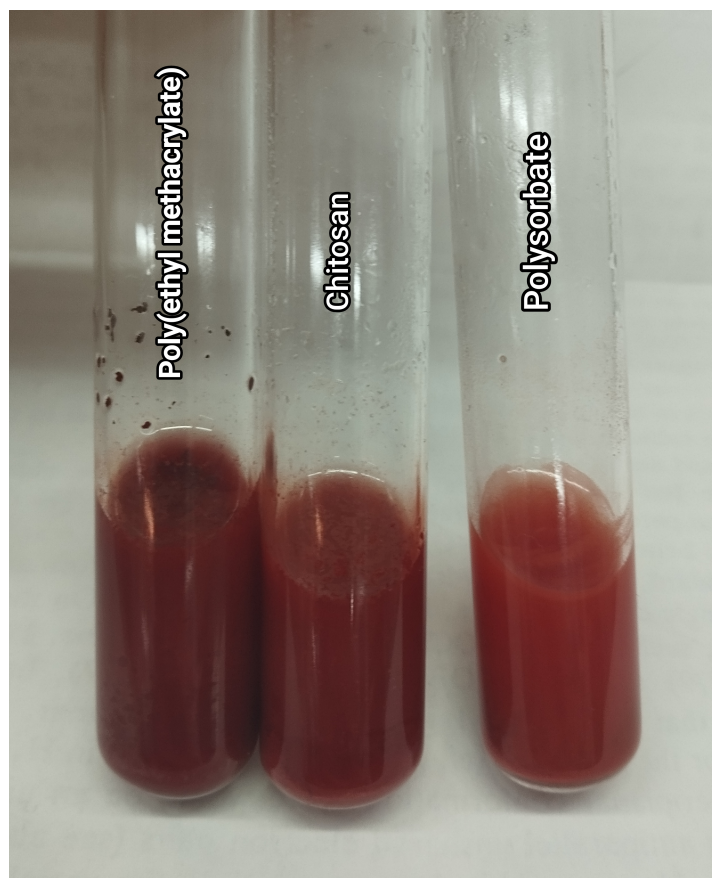


Figure S54 The reaction mixture of SeO_2 (0.5 mmol) diethylphosphite (1 mmol) with other stabilizers in water after 2h at 60 °C